

2015

MEMS graphene strain sensor

Clinton Wen-Chieh Young
Iowa State University

Follow this and additional works at: <https://lib.dr.iastate.edu/etd>

 Part of the [Electrical and Electronics Commons](#)

Recommended Citation

Young, Clinton Wen-Chieh, "MEMS graphene strain sensor" (2015). *Graduate Theses and Dissertations*. 14736.
<https://lib.dr.iastate.edu/etd/14736>

This Thesis is brought to you for free and open access by the Iowa State University Capstones, Theses and Dissertations at Iowa State University Digital Repository. It has been accepted for inclusion in Graduate Theses and Dissertations by an authorized administrator of Iowa State University Digital Repository. For more information, please contact digirep@iastate.edu.

MEMS Graphene Strain Sensor

by

Clinton Wen-Chieh Young

A thesis submitted to the graduate faculty
in partial fulfillment of the requirements for the degree of
MASTER OF SCIENCE

Major: Electrical Engineering

Program of Study Committee:

Liang Dong, Major Professor

Gary Tuttle

Mani Mina

Iowa State University

Ames, Iowa

2015

TABLE OF CONTENTS

	Page
LIST OF FIGURES	iv
LIST OF TABLES	vi
ABSTRACT	vii
CHAPTER 1: INTRODUCTION	1
1.0.1 Motivation	2
1.0.2 Outline of Thesis	3
1.1 Introduction to Graphene	5
1.1.1 Properties	7
1.1.2 Applications	9
1.2 Microelectromechanical Systems (MEMS) Strain Sensor	12
1.2.2 Graphene Based Strain Sensor	15
CHAPTER 2: FABRICATION OF A GRAPHENE BASED STRAIN SENSOR	17
2.1 Graphene Synthesis	17
2.2 Single Layer versus Multi-Layer Graphene	20
2.3 Patterning Decisions	20
2.4 Transfer Decisions	21
2.5 Final Device Design Decisions	21
CHAPTER 3: EXPERIMENT SETUP	22
CHAPTER 4: FABRICATION PROCEDURES	24
4.1 Graphene Patterning	24
4.1.1 Review of Conventional Patterning Processes	25
4.1.2 Graphene Patterning Steps	26
4.2 Graphene Transfer	31
4.2.1 Introduction to Transfer Methods	31
4.2.2 Step 1: PDMS Graphene Transfer	37
4.2.3 Step 2: Etching Initial Nickel Substrate	38
4.2.3 Raman Spectroscopy Tests	40
4.4 Flexible Graphene Sensors	42
4.4.1 Single Graphene Sensor	42
4.4.2 Stacked Rosette Strain Sensor	42

CHAPTER 5: DEVICE PERFORMANCE AND RESULTS	44
5.1 Piezoresistive Effect.....	44
5.2 Rosette Design for Multi-Directionality	45
5.3 Stacked Multi-Layered Device	48
CHAPTER 6: CONCLUSION AND FUTURE WORK	54
6.1 Conclusion	54
6.2 Future Work.....	54
REFERENCES.....	55

LIST OF FIGURES

	Page
Figure 1: Graphene Structures (Bucky Balls, Nanotubes, graphene sheets). All these different carbon structures come from graphene, a single sheet of carbon atoms in a hexagonal pattern. [17].....	6
Figure 2: In a semiconductor, the electron can only break the band gap if it gets enough energy from heat or a passing photon. However in graphene the gap is nearly non-existent. This is why the electrons in graphene exhibit such high mobility. [61]	8
Figure 3: Typical structure of a strain sensor.	15
Figure 4: CVD Multilayer Graphene Purchased from Graphene Supermarket.	22
Figure 5: OmniCure Series 1000.....	22
Figure 6: Diener Electric Plasma Cleaner Femto timer (version 1) used for graphene etching.....	23
Figure 7: Overview of Fabrication Process.....	26
Figure 8: Fabrication Process Overview.	27
Figure 9: Different Mask Designs.	29
Figure 10: Graphene Patterning Process.	30
Figure 12: Roll to Roll transfer. (26)	32
Figure 11: Scotch tape method of obtaining graphene.	32
Figure 13: Dry Stamp Transfer Method. (50)	34
Figure 14: Result of a Wet Etch transfer and A Wet Peel Transfer.	37
Figure 16: Graphene successfully transferred onto PDMS.	38
Figure 15: Graphene/Ni in metal etching solution.	38
Figure 17: Images showing the transfer process and the different patterns that could be fabricated.	39
Figure 18: Comparison of the peaks, providing evidence of successful graphene transfer.	41
Figure 19: Final Design: Stacked Rosette Graphene Sensor.	43
Figure 20: Strain Test of a Single Graphene-based Sensor	45
Figure 21: Direction of principal strain in a Rosette pattern.....	47

Figure 22: Mohr's circle diagram for strain analysis. Rosette axis superimposed on Mohr's circle for strain.....	47
Figure 23: Delta rosette.	47
Figure 24: Strain Testing Setup.	49
Figure 25: Sensor Characterization.	50
Figure 26: Multi-layer rosette strain plots measuring strain applied in Sensor 2 direction.....	51

LIST OF TABLES

	Page
Table 1: Different types of MEMS strain sensors.....	14
Table 2: Comparison of Graphene fabrication methods	17

ABSTRACT

Graphene is a two dimensional honeycomb structure of sp^2 hybridized carbon atoms that has possibilities in many applications due to its excellent mechanical and electrical properties. One application for Graphene is in the field of sensors. Graphene's electronic properties do not degrade when it undergoes mechanical strain which is advantageous for strain sensors. In this thesis, certain properties, such as the piezo-resistivity and flexibility, of graphene will be explored to show how they can be utilized to make a strain sensing device. Our original fabrication process of patterning graphene and the transfer process of graphene onto a flexible substrate will be discussed. The development of a stretchable and flexible graphene based rosette strain sensor will also be detailed.

Developing a novel, reliable patterning process for the graphene is the first step to manufacture a stretchable graphene based sensor. The graphene was patterned using a photolithography and etching process that was developed by our research team, then it was transferred to a flexible polymer substrate with the use of a combination of soft lithography and wet etching of the Ni foil with ferric chloride solution. Graphene patterning is an essential step in fabricating reliable and sensitive sensors. With this process, graphene can be consistently patterned into different shapes and sizes. To utilize the graphene as the sensing material it also needs to be transferred onto a flexible substrate. The innovative transfer process developed by our research team consistently adheres graphene to a flexible PDMS substrate while removing the original nickel substrate. In the end, the graphene was transferred from the metal substrate to the desired flexible substrate. This process was repeated multiple times to create a stack and multilayer device.

While many graphene-based strain sensors have been developed, they are uni-directional and can only measure the strain applied on the sensor in a principle direction. This issue was solved in this thesis by arranging the graphene sensors in a rosette pattern which enabled for multi-directional strain detection. The strain sensor was further improved by stacking the graphene sensors in a rosette pattern; which was possible by leveraging the advantages of soft lithography and bonding processes and the flexibility of graphene. Our final device was a stacked rosette graphene strain sensor that was able to successfully measure strain in multiple directions and magnitudes simultaneously.

CHAPTER 1: INTRODUCTION

Silicon is the most important material in modern semiconductor industries and is the material used by semiconductors that are the foundation of modern electronic technology. Research in semiconductor materials, fabrication, and other processes over the past decades has generated a steady progress in semiconducting devices; this effect is known as Moore's Law [1]. Two main factors have contributed to silicon's dominance in semiconducting devices and technologies: 1) the abundance of the element in the Earth's crust, 2) the ease of tuning the electronic, fabrication, and other properties of the material. However, due to graphene's exceptional mechanical and electrical properties, graphene has the great potential to replace silicon [2], [3]. Silicon has limitations which will hinder its applications towards flexible and large scale electronics, and this is where graphene has an advantage over silicon. Graphene also shows great promise in composite and hybrid materials in which graphene is mixed with other materials such as silicon.

Graphene is a material that has been generating interest in the microelectromechanical systems (MEMS) field due to its thinness, high carrier mobility [4], high Young's modulus [5], and numerous other properties [3]. Graphene is a single layer of Carbon atoms arranged in a hexagonal structure [2], [3] and these attributes contribute to the exceptional electronic and mechanical properties of the material [5], [6].

The possible applications for graphene are being extensively researched [3]. The potential applications are numerous from graphene replacing silicon to graphene hybrid materials. However there are very few investigations in the MEMS field for using graphene as the strain sensing material in a sensor. It has been reported that graphene has a piezo-resistance response

[7] and that it exhibits high sensitivity to strain [8]. Additionally, experiments have shown that graphene has excellent stretch ability and repeatability of stretching [9]. These properties have made graphene a good candidate for strain and strain sensing applications.

In this thesis, a Graphene-based MEMS pressure and strain sensor fabricated and patterned using a standard lithography process will be first presented as background information. The graphene strain sensor was transferred onto a thin, flexible plastic substrate after patterning. In addition a relatively simple method of patterning graphene using a standard lithography process and the method of transferring the graphene onto a flexible substrate of PDMS will be discussed. Also, the process to manufacture a multi-directional strain sensor that eliminates the limitations of a single strain gauge will be presented. The multi-directional strain sensor is manufactured by aligning 3 single strain gauges in Rosette manner to allow for measuring strain in multiple directions and magnitudes. Lastly, the consistency and repeatability of these strain sensors that are produced will be demonstrated.

1.0.1 Motivation

Strain sensors are commonly built as MEMS devices. But these MEMS devices have been limited by many factors from the rigidity of the material they are made up of, typically silicon, and the sensitivity of such sensors, to the size and thickness of the device. However with the discovery of graphene, it has opened up many applications that were not possible before.

The strain gauge has for many years been and still is the fundamental sensing element in many different types of sensors: stress, strain, pressure, torque and many other sensors. By incorporating graphene into a strain gauge, the aim is to show that graphene can be used as the sensing element in the sensor. The purpose of our device is to show that graphene can be incorporated into a strain sensor and that given its unique characteristics it can be used to

fabricate a stacked device in the shape of a rosette for improved minimization of size and accuracy of strain sensing. The common single graphene based strain sensor is only capable of detecting strain in a single direction. This problem is solved by using a rosette design to measure strain in multiple directions, however a planar rosette covers a large area and lacks the accuracy of a layered design. Our device solves both these issues by combining the rosette pattern and the stack ability of graphene to create a stacked rosette pattern graphene strain sensor. Given graphene's properties, it may replace silicon to improve the sensitivity, size, and robustness of strain sensors.

The objective of this thesis is to develop an original graphene-based stacked rosette strain sensor and to demonstrate the performance of a graphene based strain sensor.

1.0.2 Outline of Thesis

In chapter one, an introduction to the thesis and graphene will be introduced. This chapter will cover important graphene properties related to the research. These properties are presented to provide the necessary background to understand graphene-based sensors. Current conventional MEMS strain sensors will also be discussed to provide the necessary understanding of how strain sensors function. Lastly an overview of graphene based strain sensors will be covered.

Chapter two will present an overview of the research. It will discuss decisions regarding the initial graphene material, the steps in fabrication, and the final stacked rosette strain sensor. CVD graphene has two common metal substrates, nickel and copper, reasoning will be discussed as to why nickel was chosen as the initial substrate. This section will also discuss the rationale behind the fabrication decisions that were made from the patterning to transfer of graphene. An overview of the final stacked rosette strain sensing device will conclude this section.

Chapter three will detail the laboratory set up for each step of fabrication and device development. A description of the lab equipment used and the set up for the equipment will be detailed. Initial testing of materials and equipment will also be detailed in this chapter.

Chapter four will be split into multiple sections with each section covering each important step of the developed fabrication processes. This will include details on the lithography process that was developed to pattern the graphene. The developed method allowed for micro-scale patterning graphene into a variety of shapes, patterns and sizes. This section will also describe the graphene etching process and how oxygen (O_2) plasma was used. The result of this section is a patterning process that can be adapted to many different pattern designs and sizes for graphene. This chapter also covers the transfer process of graphene onto a flexible substrate. This section will also cover multiple methods of how other research groups are transferring graphene and how I developed a unique method of transferring the already patterned graphene onto PDMS. This section will also cover the use of Raman as a tool for characterizing the layers of graphene. The last section of chapter four will discuss the stackable, multi-layered graphene device that was developed. A brief introduction to graphene sensors and current devices will be covered first to provide the necessary background information. Then the individual graphene sensors and then how they were incorporated into one stacked device will be discussed.

Chapter five presents the results of our single graphene strain sensor and our stacked rosette strain device.

In chapter six a conclusion and possible paths for future work are presented.

1.1 Introduction to Graphene

Graphene is a single layer of sp^2 -bonded carbon atoms that are arranged in a honeycomb lattice as seen in Figure 1. In 2010, Andre Geim and Konstantin Novoselov were awarded the Nobel Prize in Physics for the discovery of graphene [10]. The term “graphene” was first used in 1987 to describe singular sheets of graphite as a constituent of graphite intercalation compounds, better understood as crystalline salt of the intercalant and graphene [11]. Graphene is the combination of graphite and the suffix-ene, which is used in organic chemistry to form names of organic compounds where the $-C=C-$ group is present. It is also used in inorganic chemistry to describe a one-atom thick two-dimensional layer of atoms. Hence graphene is defined as a one-atom thick two-dimensional layer of carbon atoms. However this term has also been used in early descriptions of carbon nanotubes [12], but true graphene really is a two-dimensional single atom thick layer of carbon atoms. It is the first two-dimensional crystal structure available to us and this opens up a lot of possibilities in the world of science and technology.

Graphene is a material that was argued it could not exist theoretically 70 years ago because a 2D material is too thermodynamically unstable. Thermal fluctuations in such a low-dimensional material would lead to too great of displacement of the atoms [13], [14]. This theory by N. D. Mermin and H. Wagner was known as the Mermin-Wagner Theorem [15] and was supported by experimental observations that showed the melting temperature of thin films decreased as the thickness of the film decreased and the film became increasingly unstable. However this “academic” material was discovered. That is why graphene is known as the “miracle material.” When free-standing graphene became a reality, massive efforts toward its research began in earnest [16].

The main reason there is an abundance of research going into graphene is its many potential applications [17], [2]. In 2004, the Geim group reported that the carrier density in graphene can be controlled by the application of gate voltage. Therefore in graphene based electronic devices the concentration and mobility of the charge carriers can be manipulated with the application of voltage [18]. Currently the miniaturization limit of silicon based electronic devices is 50 nanometer long electrical channels for carrier transport [19]. Graphene on the other hand has been successfully shown that the transportation of charge carriers occurs even in graphene strips only a few nanometers long [2]. This means that the miniaturization of electronic devices can be further improved by using graphene based electronic devices and circuits.

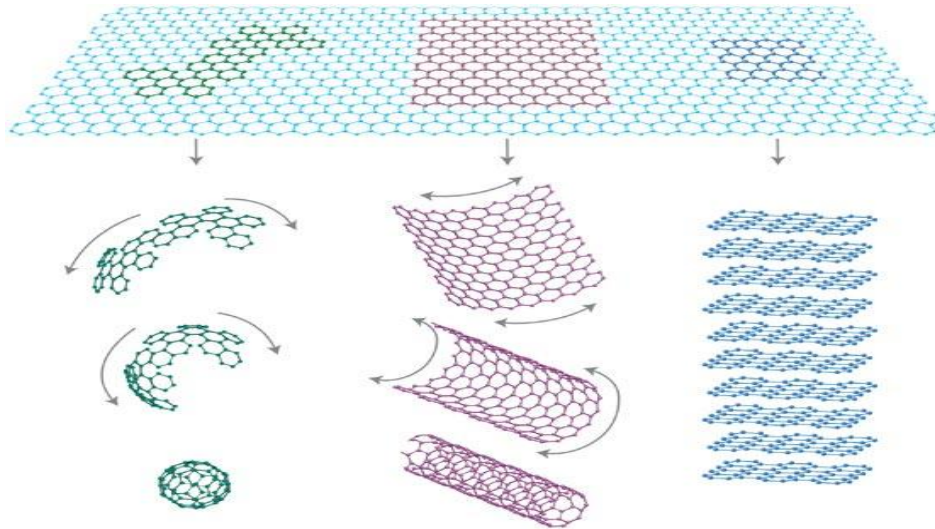


Figure 1: Graphene Structures (Bucky Balls, Nanotubes, graphene sheets). All these different carbon structures come from graphene, a single sheet of carbon atoms in a hexagonal pattern. [17]

1.1.1 Properties

1.1.1.1 Electronic

To understand graphene's electrical properties one must first understand the importance of the honeycomb lattice structure of the carbon atoms. Each carbon atom has 6 electrons, two in the $1s^2$ orbital and the other four in the outer valence shell in the 3p states [20]. The individual σ bonds are at 120 degrees and this is the reason for the hexagonal structure of graphene. The σ bond is a strong covalent bond, and this bond strength is why graphene shows excellent mechanical properties [5].

The linear E-k relationship in graphene leads to zero effective mass for electrons and holes [21]. Therefore the carriers in graphene are essentially relativistic particles such as photons and follow the Dirac equation instead of Schrodinger's. Electron mobility at room-temperature is $2.5 \times 10^5 \frac{cm^2}{V*s}$, with the theoretical prediction of $(\sim 2 \times 10^5 \frac{cm^2}{(V*s)})$. Graphene in its pure state has no energy band gap which is an issue if this material is to be used in transistor applications, but there is research indicating a band gap can be induced. Electrons exhibit high mobility at the range of $\frac{200000cm^2}{V*s}$ with current densities of $2 \times 10^{11} cm^{-2}$. In comparison silicon has an electron mobility of $15,000 \frac{cm^2}{V*s}$ [22]. However these properties are only maximized for the highest quality of graphene, but as fabrication process improve, the characteristics will be achieved with a variety of graphene.

1.1.1.2 Graphene compared to traditional materials

Band gap: Semiconductors traditionally have a finite band gap, hence the name semiconductor, but graphene does not have any natural gap as shown in Figure 2. There has been research showing that it is possible to induce a band gap in graphene that will be useful for the transistor

application. Typically the study of electron and hole motion of semiconductors is done with different doping materials. However for graphene, the nature of the charge carriers changes at the Dirac point from a hole to electron and vice-versa. The Fermi level of semiconductors often fall within the bandgap, but in graphene the Fermi level is always within the conduction and valence band.

Linear dispersion relation: Most semiconductors have a dispersion relation that is quadratic, but graphene shows a linear dispersion relation near the Dirac points. Several important electronic properties are explained by the electronic band structure of graphene.

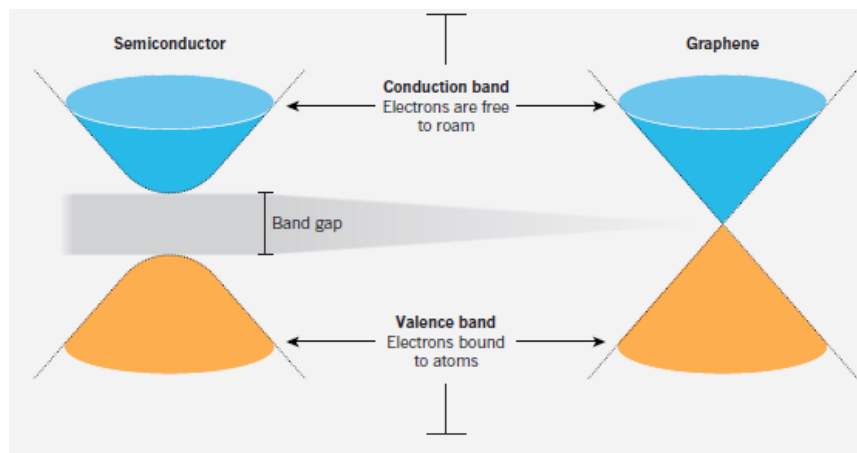


Figure 2: In a semiconductor, the electron can only break the band gap if it gets enough energy from heat or a passing photon. However in graphene the gap is nearly non-existent. This is why the electrons in graphene exhibit such high mobility. [61]

1.1.1.3 Mechanical

Because graphene is a two-dimensional material, it is easy to change the distance and angles of the carbon atoms that also induce changes in electron behavior in graphene. Therefore graphene is an ideal material for sensing applications. Graphene is a two-dimensional film with a thickness of 3 angstroms and, thus makes it the thinnest material which is vulnerable to

distortions caused by thermal fluctuations. These distortions occur because of the change in distance and relative angles between the carbon atoms. Three dimensional materials do not suffer from these kinds of distortions. Therefore to utilize the benefits of graphene to its fullest extent, forming a 3D graphene structure is suggested.

1.1.2 Applications

The potential applications of graphene are being actively explored, and given the phenomenal properties in the material the possibilities are very open. Graphene will garner even greater interest outside of academia once mass-producible high quality graphene become available. This thesis will discuss a few of the major areas that are currently being explored.

1.1.2.1 Graphene based electronics

Graphene shows great potential in the future of electronics from electrical circuits to transistors. Because the conduction and valence bands are separated by zero band gaps, it makes the electrical and structural properties extremely desirable. The zero band gap feature create high mobilities and enables high frequency devices [3]. Carrier mobilities up to the range of $20000 \frac{cm^2}{V*s}$ have been reported in single and multilayer graphene. Graphene films that are suspended have reported mobility that exceeds $\frac{200000cm^2}{V*s}$ [22]. These extremely high carrier mobilities mean that graphene transistors will have fast operating speeds. Graphene thin film transistors (TFTs) also show large current densities ($\sim \frac{2x10^8 A}{cm^2}$) [23] and high saturation velocity ($\sim 5x10^7 \frac{cm}{s}$) [24]. Experimental predictions show that graphene's saturation velocity can be twice as high as GaAs and possibly four times that of silicon. This is important because as the sizes of the devices continue to shrink into the nanometer scale, the saturated carrier velocity becomes a more important measure of the transport properties [25]. Graphene may be

the next step in miniaturizing electrical devices and systems. However the fabrication of graphene based devices is still an obstacle that must be overcome.

1.1.2.2 Flexible Electronics

Flexible electronics require low sheet resistance with high transmittance (>90%) depending on the application. Graphene meets these electrical requirements and has excellent mechanical flexibility and durability, which are also very important properties for flexible electronic devices [26]. Traditionally indium tin oxide (ITO) is the material used, but it is expensive. With the improvements in graphene fabrication and its quality, graphene has a good chance of replacing ITOs in the future.

1.1.2.3 Transistor

Graphene is predicted to start having a major impact in the transistor industry after 2020. Currently, the main issue is that graphene does not have a bandgap required in transistors. But there is much research going into solving how to induce a bandgap in graphene by nanoribbons, chemically modified graphene, and bilayer control. However currently these methods have been unable to meet the required 10^6 on/off ratio needed in a bandgap. Worst of all is the fact that these methods of inducing a bandgap leads to degradation of carrier mobility in graphene. The transistor application with graphene still needs more research before it can be fully realized.

1.1.2.4 Composite/hybrid material

The mechanical, electrical, chemical, and barrier properties of graphene make it an ideal material for composite material applications. Composite materials are becoming more significant in the design of some future applications such as vehicles, infrastructure, and other applications that require high strength with extremely light weight materials. Currently carbon fiber is a popular material used in numerous applications such as sports cars because it is

extremely light and strong. Carbon fiber is just a derivative of graphene in a less pure form. Carbon fiber is the combination of carbon fibers mixed with polymers such as polyester or nylon. The introduction of graphene to composite polymers could increase the temperature resistance of the polymer, induce an antistatic behavior, improve compressive and tensile strength, reduce moisture uptake, and give lightning protection. Graphene also offers better properties in certain applications over carbon fibers given its excellent mechanical properties [27]. Currently in polymer composites an important factor is the strength of the link between the polymer and its additives. Due to the surface defects, the wrinkled surface of graphene makes for extremely strong bonds with polymer materials. This will enhance the interfacial load transfer between the polymer materials and graphene.

Even though graphene is regarded as a perfect 2D lattice of carbon atoms, there may be many different applications for non-uniform or defected graphene. Research in graphene continues to grow rapidly and as graphene is exposed to more disciplines, this will lead to faster integration of graphene into many more applications.

1.2 Microelectromechanical Systems (MEMS) Strain Sensor

A strain gauge is a device that measures strain and is commonly fabricated using various materials and semiconductors. A strain gauge works by having a flexible backing that supports a metallic foil pattern. This gauge is attached to an object and as that object is deformed, the foil also undergoes deformation which caused the electrical resistance of the foil to change. The resistance R can be written as

$$R = \rho * L / S \quad \text{Eq. 1}$$

Where ρ is the resistivity constant of material; L is the length; S is the average cross-sectional area.

When strain is applied, the resistance changes and this effect is known as piezoresistivity. The relation between the change in electrical resistance and the strain is represented by the equation

$$\text{GF (gauge factor)} = (\Delta R / R) / \epsilon \quad \text{Eq. 2}$$

Where $\Delta R / R$ is the normalized resistance variation; ϵ is the mechanical strain.

The first piezoresistive silicon pressure sensor and strain gauges which developed into Micro-electromechanical systems (MEMS) was described by Charles Smith from Bell Labs [28]. Piezoresistance is the effect where the resistance change with the applied strain, this phenomenon is fundamental in MEMS sensing. The term MEMS does not only describe electromechanical devices nor does it only describe “systems”. MEMS is widely used to describe all manner of miniaturized devices, most fabricated from silicon and using microelectronic industry techniques. Today, many devices are all referred to as MEMS: silicon microsensors, “Lab-on-chip”, or micro-total analytical systems.

MEMS technology has been very successful in the field of physical sensing and has yielded many small, robust, and inexpensive devices such as strain gauges, pressure sensors, accelerometers and gyroscopes. MEMS piezoresistive strain sensors offer advantages such as high sensitivity [29], good scaling characteristics, low cost, and the ability to have detection electronics circuit on the same sensing board. Today's devices can be exceedingly small and most utilize piezoresistive effects for sensing. Since pressure sensors are in many applications from medical, aerospace to automation and control, the impact of MEMS sensors is great.

Typical types of MEMS sensors include, but not limit to, the following:


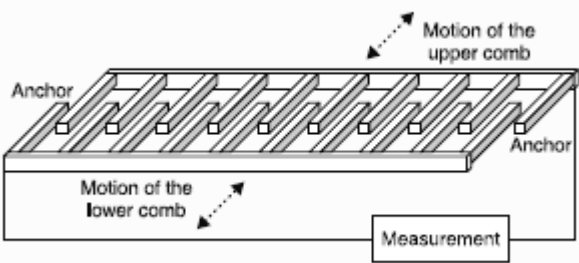
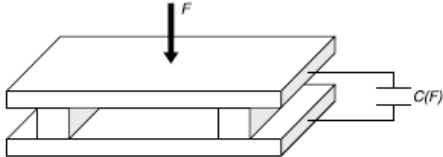
Strain gauges: Strain gauges work by transducing a mechanical signal into an electrical signal. This can be done by measuring the change in resistance of a metal conductor undergoing strain, this is a piezoresistive strain gauge. Fiberoptic strain sensors sense the change in wavelength or phase of light which is also a measure of strain [62].

Capacitive detection: Variation in capacitance caused by electrode motion changes the mechanical signal to an electrical signal in capacitive detection. This method offers the advantage of smaller size, higher sensitivity and lower power compared to piezoresistive measurements [62].

Pressure sensor: By combining bulk micromachining and wafer bonding, small, robust micro membranes can be produced. Pressure sensors can also be produced with surface micromachining and capacitive detection to measure the variation in the small membrane [62].

There are many different types of MEMS strain sensors, shown in Table 1, each with their own advantages and disadvantages.

Table 1: Different types of MEMS strain sensors.

<p><i>Strain gauges:</i> Strain gauges work by transducing a mechanical signal into an electrical signal. This can be done by measuring the change in resistance of a metal conductor undergoing strain.</p>	<p>Common image of a MEMS strain gauge structure [62].</p> 
<p><i>Capacitive detection:</i> Variation in capacitance caused by electrode motion changes the mechanical signal to an electrical signal in capacitive detection.</p>	<p>Example of a capacitive sensor [62].</p> 
<p><i>Pressure sensor:</i> By combining bulk micromachining and wafer bonding, small, robust micro membranes can be produced.</p>	<p>Example of a pressure sensor [62].</p> 

1.2.1 Graphene Based Strain Sensor

1.2.1.1 Mechanisms of graphene strain sensor

A typical structure of a graphene strain sensor is depicted in Figure 3. When strain is applied, a resistance change can be measured or as depicted in the figure, if voltage is applied across the strain sensor, current change can be measured. The graphene device developed by our research team can be categorized as a strain sensor that is based on structural deformations. The strain that leads to elongation of our graphene will cause a shifting in the electrical band structure and results in changes in the electrical properties. The change in resistance is explained by the distortion of the hexagonal honeycomb crystal structure of graphene, as strain is increased the resistance increased as well.

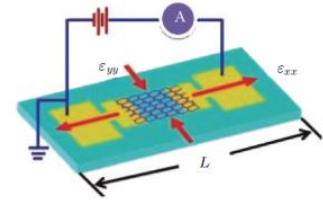


Figure 3: Typical structure of a strain sensor.

The strain sensing market is continually growing and there is a drive for miniaturized and inexpensive devices. However traditional semiconductor devices are facing limitations and this has driven research into other nanoscale materials. One material that has attracted a great amount of attention is graphene. A major advantage of graphene sensors is their ability to be multi-functional. It has been theorized that a single graphene device could be used to take multiple measurements simultaneously, for example a sensor that can measure strain, pressure, and electric field [3]. A device that is capable of multi-functionality will be very attractive to industry and consumers alike. The multi-functionality is due to the fact that graphene as a 2-dimensional material has properties that make it extremely sensitive to the environment [3]. Graphene is also the only crystal that can be stretched by 20%, thus making the working range of a graphene sensor greater than any current material.

One of the promising applications of graphene is in microelectromechanical systems (MEMS). The properties of graphene, specifically the high Young's modulus of 1TPa [5],

excellent electrical conductivity [30], extreme flexibility and stretch ability [7], are all crucial for making a graphene-based flexible sensor. The fact that the resistivity of graphene changes linearly with applied strain [31], [7] makes it an ideal material for sensing applications.

1.2.1.2 Flexible sensors

One property of graphene is that it is the strongest material ever measured, it can sustain up to 25% in-plane tensile elastic strain [9]. This strain leads to a significant lengthening of graphene, which is likely to cause a shift in its band structure and cause changes in the electrical properties. Typically in a flexible sensing device, the semiconductor substrate is replaced with a support that is softer and more flexible like plastic or steel. Even though there are well established fabrication processes for thin-film devices, there are still several problems that need to be solved regarding flexible substrate devices. When dealing with flexible substrates, the process is very temperature dependent. Most approaches using amorphous silicon, organics, and polycrystalline silicon are low temperature processes. However these materials usually have high defect densities and low carrier mobilities. Graphene on the other hand is extremely flexible and has an extremely high mobility and can withstand high temperatures.

Though graphene-based strain sensors have garnered much attention for their potential in miniaturized and high-performance strain sensors, they still have a long way to go before a commercial strain sensor is realized. Research in this field has been rapid and recently been focused on creating a higher sensitivity and more stable graphene-based sensor. Such a sensor has many potential applications such as touch screens or in biological applications as a bridge from electrical to biological. However for an established material to be replaced, the properties of graphene must be able to translate into applications that are competitive enough to justify cost and change of existing processes.

CHAPTER 2: FABRICATION OF A GRAPHENE BASED STRAIN SENSOR

Our initial research efforts were focused on developing a reliable patterning process for the graphene. The graphene was patterned using a photolithography and etching process that was developed by our research group. The next step is to develop a method of transferring the patterned graphene onto a flexible substrate and remove the initial metal substrate. Once the patterned graphene was transferred onto the flexible substrate, at this point a uni-directional strain sensor was created. However the aim of this thesis was to create a strain sensor that could measure in multiple directions, but instead of using a planar rosette design our sensor was a stacked rosette strain sensor which gave our device added benefits.

First a decision had to be made regarding what kind of graphene was to be used in this research.

2.1 Graphene Synthesis

There are four primary methods which are widely used to fabricate graphene, as shown in Table 2: mechanical exfoliation, chemical vapor deposition (CVD) growth on a metal substrate, high-temperature annealing of SiC, and chemical reduction of graphene oxide. The advantages and disadvantages of each fabrication method will be summarized below to explain why CVD

Table 2: Comparison of Graphene fabrication methods.

Method	Crystallite size (μm)	Sample size (mm)	Charge carrier mobility (at ambient temperature) ($\text{cm}^2\text{V}^{-1}\text{s}^{-1}$)	Applications
Mechanical exfoliation	>1,000	>1	$>2 \times 10^5$ and $> 10^6$ (at low temperature)	Research
Chemical exfoliation	≤ 0.1	Infinite as a layer of overlapping flakes	100 (for a layer of overlapping flakes)	Coatings, paint/ink, composites, transparent conductive layers, energy storage, bioapplications
Chemical exfoliation via graphene oxide	~ 100	Infinite as a layer of overlapping flakes	1 (for a layer of overlapping flakes)	Coatings, paint/ink, composites, transparent conductive layers, energy storage, bioapplications
CVD	1,000	$\sim 1,000$	10,000	Photonics, nanoelectronics, transparent conductive layers, sensors, bioapplications
SiC	50	100	10,000	High-frequency transistors and other electronic devices

graphene was chosen by our research team as the base material to be used.

Mechanical exfoliation was the first successful method of producing graphene [10]. Graphene was first discovered by exfoliating graphite layers with tape and isolating these layers until a single layer of graphite was left. This method became famously known as the ‘Scotch Tape Method’ [10]. Other methods of mechanical exfoliation involve using tweezers to remove layers of graphite from a bulk crystal source. In terms of structural stability, mechanical cleaving of a graphite source provides the best quality of graphene. Using mechanical exfoliation it is possible to obtain monolayer or multiple layers of graphene. The best quality of graphene in terms of crystallite size and mobility is obtained using this method, but sample sizes are typically small, less than 1mm. This method was used at the start of the research to extract graphene from the metal substrate it was grown on.

High-temperature annealing of SiC involves the evaporation of the silicon at extremely high temperatures leaving only the carbon layers which forms graphene [32]. Silicon carbide is a common material in high-power electronics. However this method is not widely used due to the high cost of the initial SiC wafer and that high temperatures in excess of 1000 degrees Celsius are needed. This technique may be limited for high frequency devices where excellent performance of devices will offset cost.

Graphene Oxide (GO) can also be chemically or thermally reduced into graphene. Graphene Oxide is made by oxidizing pure graphite powder with subsequent sonication [33]. This GO is then spin coated onto some arbitrary substrate to form a large scale continuous film. However graphene oxide has a high concentration of oxygen defects making GO an electrical insulator. Therefore graphene oxide must be reduced into graphene to restore the desired electrical properties in graphene. GO can be thermally reduced at low temperatures in an argon

flow or chemically reduced using hydrazine [34]. However this does not completely convert GO into graphene, some oxygen remains in the graphene at a ratio of approximately carbon to oxygen 10:1 [33]. Reduction of GO produces the largest area of graphene but the quality is also the worst compared to the other fabrication methods.

Chemical vapor deposition (CVD) is a method of growing graphene that shows the most promise, is relatively inexpensive and is a readily accessible approach of fabrication. Reasonably high quality graphene is chemically vapor deposited onto a metal substrate such as nickel or copper. Chemical Vapor Deposition works by having a carbon-bearing gas that reacts to a metal catalyst in high temperatures (800-1100 degrees Celsius). The mechanism of graphene growth on metal is influenced by several factors: carbon solubility, crystal structure, lattice parameters, the metal and thermodynamic parameters such as pressure and temperature of the system. Graphene growth on nickel (intermediate solubility metal) is a combination of carbon atom diffusion into a metal at a specific temperature and carbon atoms segregation from the bulk to the metal surface during cooling after the CVD process. Graphene growth on copper (low carbon solubility material, 0.001 atomic %), is limited to the surface of the metal; this is why graphene on copper is typically limited to one or two layers. Copper has received more attention compared to other metal substrates because of three main reasons: 1) it has very low solubility with carbon, 2) if copper film is annealed around its melting temperature; the grain size growth is that of large uniform graphene, 3) it is more flexible at low thicknesses.

In respects to graphene fabrication, the main goal is to find a method that is low cost and able to synthesize high quality graphene on a large scale for industry uses. The decision was made by the research team to use CVD graphene due to its ease of fabricating large scale, multilayer sheets of graphene with good electrical and mechanical properties. Some of the

different CVD graphene choices and an explanation why the final decision was to go with graphene grown on a nickel substrate will be discussed below.

2.2 Single Layer versus Multi-Layer Graphene

It is possible to control how many layers of graphene are grown on the metal substrate using CVD. Single layer to bilayer graphene is most commonly grown on copper using CVD, the layers are limited because CVD graphene is a self-limiting process and copper has a low carbon solubility leading to only growing graphene on the surface of copper [35]. Single layer graphene is almost 100% optically transparent and therefore Raman spectroscopy is needed to test for the evidence of graphene, especially post-transfer onto a transparent substrate like PDMS. Single layer graphene shows the best electrical properties compared to multi-layered graphene, this is because single layer graphene is most similar to pristine graphene which exhibits the best characteristics. However single layer graphene is difficult to work with in respect to our research because the graphene undergoes many processing steps that weaken and etch away graphene layers.

Nickel is a common metal substrate for CVD graphene when multiple layers are desired. Graphene grown on nickel can reach layers numbering in 300 monolayers. Graphene has an incredible absorption of incident visible light of 2.3% [36]. This makes graphene extremely transparent and invisible to the naked eye, therefore by having many layers, this made graphene less transparent and easier to manipulate and work with, while maintaining the phenomenal properties of graphene.

2.3 Patterning Decisions

There is research in which groups have successfully used e-beam lithography to etch graphene, for this reason the decision was made to try photolithography to achieve graphene

patterning. However the use of photolithography dictated that an additional etching step would be required to etch the graphene. Etching was done with an oxygen plasma etcher, these fabrication steps will be further detailed in later chapters.

2.4 Transfer Decisions

Transferring graphene and maintaining the integrity of the material is a complicated procedure. Adding to this already difficult process was the fact that our graphene was patterned and not a solid sheet. Thus, a process of using a PDMS stamp for support and as the final substrate combined with a chemical wet etch to remove the initial metal substrate was developed to achieve a reliable, stable and robust transfer method.

2.5 Final Device Design Decisions

In the field of strain sensing, the rosette pattern is commonly used because it allows for multi-directional strain sensing. A strain gauge rosette is an arrangement of two or more closely positioned gauges. In common cases where the principal directions of strain are unknown, all it takes is three independent strain measurements (all of different directions) to determine the principal strains. Due to the flexibility of graphene, it is possible to stack our devices to form the rosette pattern and this is advantageous over current planar rosette sensors. A stacked rosette minimizes sensor size yet is still able to measure multiple directions and magnitudes of strain to a very precise point.

CHAPTER 3: EXPERIMENT SETUP

Our research lab is located in Coover Hall at Iowa State University in Ames, Iowa. Our lab consisted of 3 different sections: a photolithography area, a chemical processing area, and a main general lab area, all located on the 1st floor of Coover Hall.

The CVD graphene used by our research team was purchased from Graphene Supermarket, as shown in Figure 4. It was about 300 monolayers of graphene at ~105 nanometer thickness on a 2"x2" square nickel substrate [37].



Figure 4: CVD Multilayer Graphene Purchased from Graphene Supermarket.

Photolithography: AZ5214 was the photoresist used for patterning and deposited on the graphene. AZ 5214 is a positive photoresist that becomes soluble when exposed to ultraviolet light exposure and thus can be removed using developer. The developer used was AZ 726, post exposure the entire graphene/nickel sample was placed in the developer solution and soaked to remove specific areas of photoresist. Photolithography was done with an OmniCure Series 1000, as shown in Figure 5.



Figure 5: OmniCure Series 1000.

Graphene etcher: Oxygen plasma etching, it involves producing plasma from a process gas, in our case oxygen, and using a high frequency electric field to convert the gas into plasma. The plasma is the etching element that etches away the exposed graphene. Our lab has a diener electric Plasma cleaner Femto timer (version 1) as shown in Figure 6.

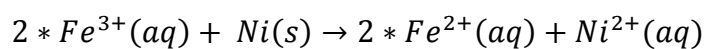


Figure 6: Diener Electric Plasma Cleaner Femto timer (version 1) used for graphene etching.

PDMS stamp: Sylgard 184 Elastomer kit was used to fabricate the PDMS stamp and the flexible substrate for the graphene. The kit is a combination of Base and Curing Agent. The curing agent is mixed with the Base so that the Base polymers cross-link and solidify creating a solid polymer. The critical factor in the PDMS stamp is the ratio of Base to curing agent, it must be 15:1 Base to curing agent. The importance of this will be discussed later in this thesis.

Metal etching solution: The nickel etching solution was made with ferric chloride hexahydrate and de-ionized water. The ferric chloride solution was prepared with 27 grams of ferric chloride and 300 ml of DI water or (~0.1 g/ml).

An aqueous iron (III) chloride (FeCl_3) solution (1 M) was used as an oxidizing etchant to remove the nickel substrate. The net ionic equation of the etching reaction is:



CHAPTER 4: FABRICATION PROCEDURES

4.1 Graphene Patterning

When Andre Geim and Kostya Novoselov first isolated the atomically thin film of graphene in 2004, by exfoliating monolayers of graphite with scotch tape [38], it was an unpatterned sheet of graphene. Even then it was clear that graphene has immense potential in future technological applications. This interest in graphene stems from the unique electronic structure of the material. As a truly two-dimensional material, the electronic states of graphene are different from conventional semiconductors. However by examining the evolution of silicon based technologies, it can be seen that it is not just the intrinsic semiconducting properties that drive progress into the industry sector, but more importantly it is the control of the properties and shape. The ability to fabricate high quality complex patterns at an affordable cost is an essential driving factor. The fact that a flat wide sheet of graphene is intrinsically a semimetal, which is difficult to directly apply to semiconducting devices, means that graphene must be patterned. The ability to pattern graphene into finite structures with nanometer-scale confinement is important for tuning the transport properties of graphene-based devices. Therefore it is essential to learn how to create patterned structures in graphene, in doing so it allows for the control of graphene properties.

The research of patterning graphene is a new field that has not been heavily explored. Most current methods of patterning graphene involve breaking the C-C bonds, whether by chemical reactions, high temperature treatments, or irradiation with high-energy electrons. For this reason most research in graphene still use graphene sheets as the sensing device, the graphene is typically suspended over a cavity or made into nanoribbons. However, for a device to be made up of graphene, it needs to be patterned instead of just being a sheet. A review of

recent progress in patterning graphene will be presented first and then our method of patterning will be detailed.

4.1.1 Review of Conventional Patterning Processes

Direct cleavage is a process of directly carving mono or multilayers of graphene. However in order to create patterns on graphene by cleaving the carbon bonds, high energy energetic cleaving tools are needed. The energy it takes to cleave an atom from a graphene lattice is estimated to be ~ 17 eV [39], so the energy required to cleave a single carbon bond is about 5 to 6 eV. These processes include mechanical cleavage, probe lithography, ion beam lithography, plasma etching, chemical etching, and nano-imprint lithography [17], [40], [41]. However such a process leaves unwanted defects because of the high energy required.

Lithography methods have been used to successfully create graphene structures with pre-designed patterns. These methods can be used to create nanoribbons of graphene (GNRs). This method uses e-beam lithographical negative resist to form a protective pattern on graphene; it is then exposed to oxygen plasma which chemically removes the unprotected parts of graphene [42], [43]. Using this method it is possible to modify the band gap of graphene nanoribbons by fabricating them into different widths [44]. Such methods have a high degree of control over the “printed” patterns. The feature size and edge resolution of these methods are only limited by the instruments, and e-beam resolution depends on the e-beam size and the scattering and propagation of the electrons in the resist. Feature sizes as small as 10 nm can be achieved [43].

There are varying methods for patterning graphene depending on what kind of graphene patterning is desired. Our research team conducted an investigation into patterning methods to determine what kind of pattern was needed, equipment and resources on hand, and the final device that we are fabricating.

4.1.2 Graphene Patterning Steps

The following sections detail the steps required to pattern a graphene based strain sensor.

The processing diagram of our graphene fabrication method is show in Figure 7 and 8.

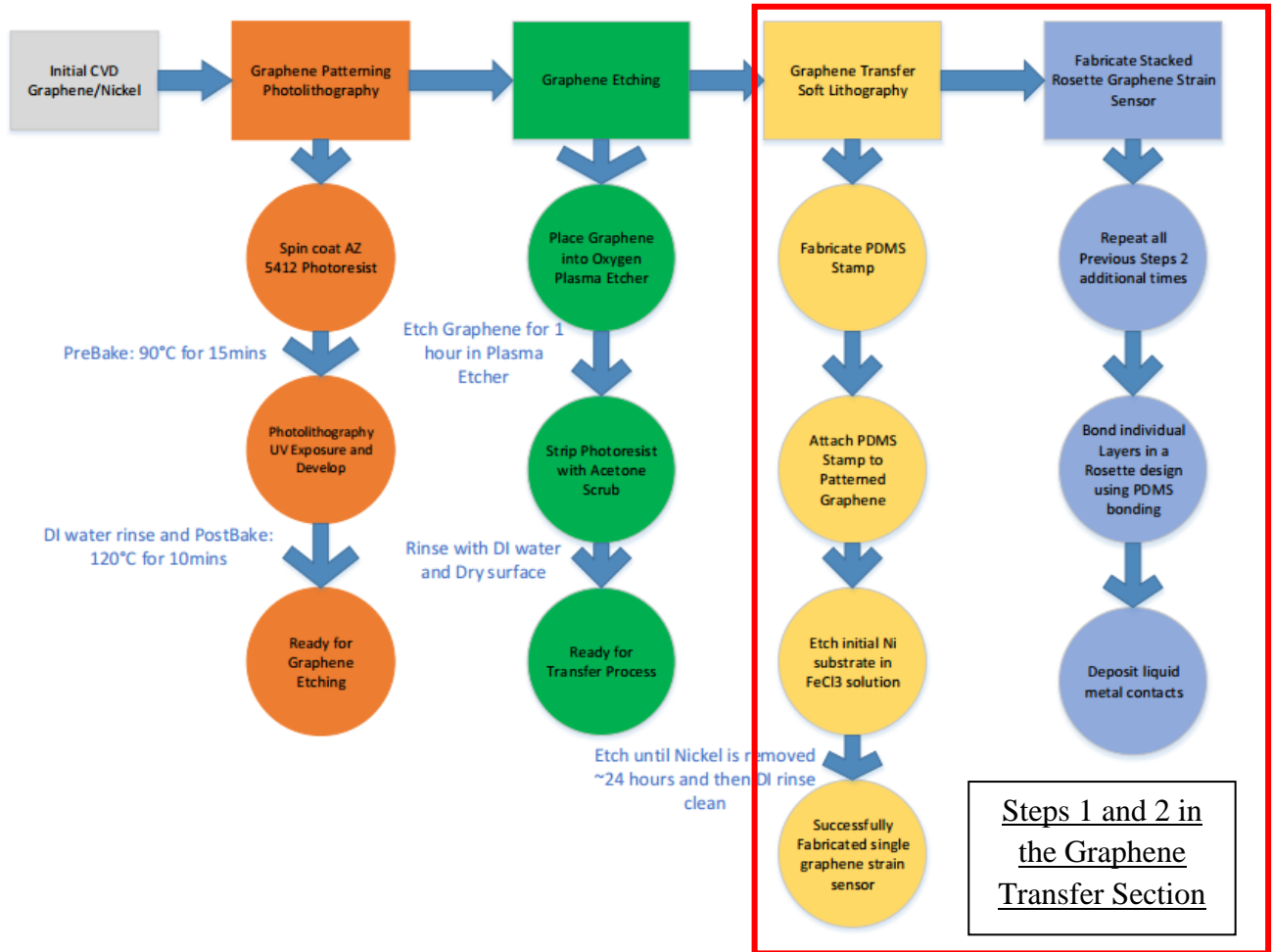


Figure 7: Overview of Fabrication Process.

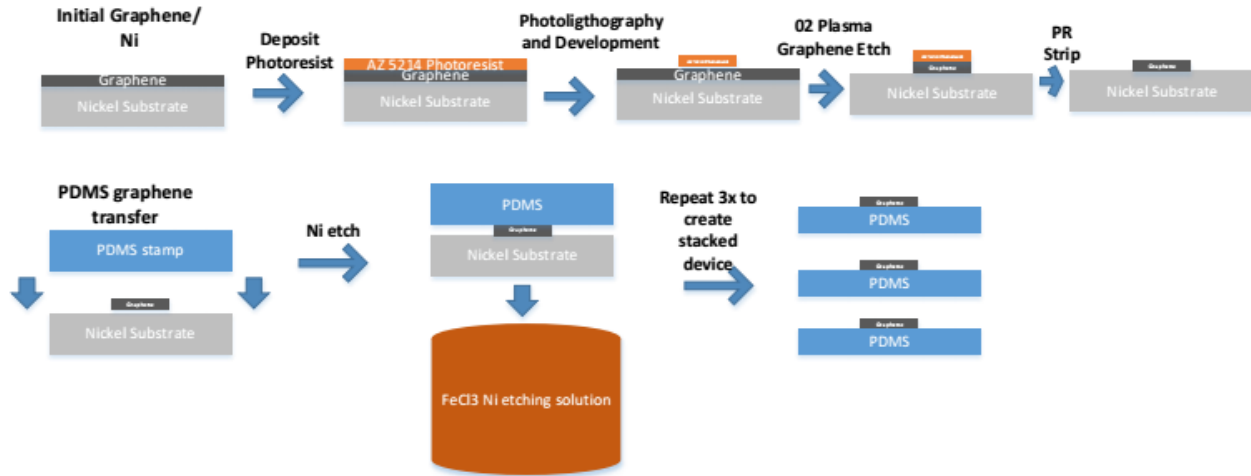


Figure 8: Fabrication Process Overview.

4.1.2.1 Step 1: Patterning Graphene using Photolithography

Photolithography, also known as optical lithography or UV lithography, is a typical process in the semiconductor industry and used in microfabrication to pattern parts of thin films or the bulk of a substrate. There is some literature in which e-beam lithography is used as a method of etching graphene; therefore the decision was made to utilize this photolithography to pattern the graphene for the device. There were many adjustments that needed to be made to the conventional lithography process to make it suitable for our process. The main obstacle was how to coordinate the lithography patterning process with the graphene transfer process. Should the graphene be transferred first onto the flexible substrate then patterned or should the graphene be patterned first then transfer the patterned graphene onto the flexible substrate. To answer this question, a determination of the transfer process had to be made first. The transfer process will be discussed more in a later section, but it was concluded that patterning graphene first then

transferring the pattern graphene had the highest rate of success after many experiments and trials.

The photolithography process begins by depositing a photoresist to form and protect the desired pattern on the graphene. The initial CVD graphene on nickel was spin coated with the photoresist AZ5214 at a rate of 500 rpm for 25 seconds, this spin speed ensured a layer of ~10 μm of photoresist that will be used to protect the graphene during the etching process. A thick layer of photoresist was needed because graphene is a tough material to etch due to the strength of its carbon bonds, therefore etching was a long process and the photoresist needed to resist through the etching process to protect our pattern graphene. After the thick layer of photoresist was spin coated onto the graphene a pre-bake process followed; the sample was baked at 90 degree Celsius for 15 minutes to drive off excess photoresist solvent and to harden the photoresist.

The next step the photolithography process is ultraviolet (UV) light exposure of the photoresist. There are two different kinds of photoresist and they have different behaviors when exposed to UV light. AZ5214 is a positive resist; this means the exposed parts of the photoresist become soluble to photoresist developer after exposure. Negative photoresist behaves in the opposite manner; the exposed parts of resist become insoluble in developer. The use of a mask, such as the ones shown in Figure 9, determines which parts of the resist are left exposed and which parts are left unexposed during the UV exposure. The mask also determines the desired pattern that will be etched into the graphene. The mask is aligned with the graphene and places everything in the UV exposure area. The photoresist covered graphene is then exposed to intense UV light for 90 seconds at $2\text{mW}/\text{cm}^2$, this causes a chemical change in the exposed areas of photoresist so that it becomes soluble to be removed by the developer solution. The

graphene is then submerged into photoresist developer, to remove the exposed areas of photoresist, and developed for 2 minutes and 30 seconds. The development time is determined by the thickness of the photoresist and due to the thick layer of photoresist, a long developer time is needed to ensure complete removal of photoresist for etching process. Post-bake or hard-baking process of 120 degrees Celsius for 10 minutes reinforced the photoresist to make it more resistant to the O_2 plasma etching process used for etching graphene.

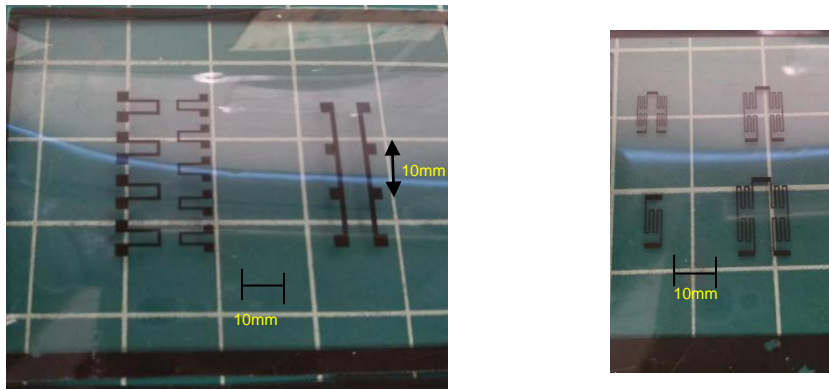


Figure 9: Different Mask Designs.

4.1.2.2 Step 2: Etching of the Graphene

Early studies into graphene etching used chemical wet etching, the graphene surface was coated with zinc and dissolving the zinc with dilute acid, this removed layers of graphene [45]. However this chemical etching created many defects in the graphene and was incompatible with the other microelectronic fabrication processes. Al-Mumen in [46] reported that by carefully tuning certain variables (power, oxygen flow rate, pressure, and time) of oxygen plasma etching, they were able to achieve layer by layer etching of graphene. They were also able to etch graphene using both oxygen reactive ion etching and oxygen plasma etching. However a smaller amount of defects are introduced to the graphene when using oxygen plasma as opposed to reactive ion etching [46].

For the fabrication procedure, detailed in Figure 10, the graphene etching is done with an O_2 oxygen plasma etcher Diener electric. Plasma etching is commonly used in semiconductor fabrication; it involves producing plasma from a process gas, in our case oxygen, and using a high frequency electric field to convert the gas into plasma. The graphene is placed in the plasma etcher, the air is vacuumed from the chamber, and then oxygen is flowed at a low pressure into the chamber and excited into plasma through dielectric breakdown. Process settings for the plasma etching were: 100% power, 8sccm (standard cubic centimeter per minute) oxygen flow rate, oxygen pressure of 8Pa. The graphene etching process took 1 hour. Following the etching process, the photoresist had to be removed from the graphene and the graphene was also removed from the silicon wafer base that it was attached to during this process. The use of acetone stripped away the photoresist on the graphene pattern and the resist holding the graphene to the silicon base. After a rinse to clean the surface of the graphene, it is now ready for the transfer process.

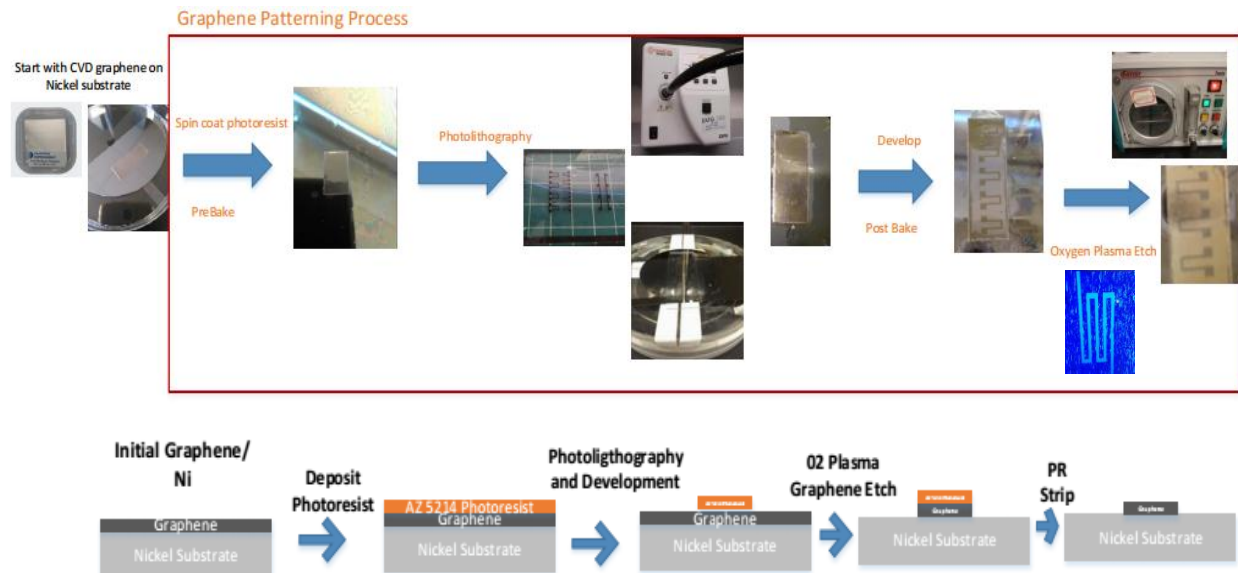


Figure 10: Graphene Patterning Process.

The unique aspect of our patterning process is that with a change of the mask it is possible to create different patterns, sizes, and shapes on the graphene. Research focused on graphene patterning, the patterns are typically micron to millimeter sized feature sizes, and it is easier to pattern on a bigger scale for large-scale graphene work. This makes our patterning process adaptable to many research applications. Our method makes vast improvements to current methods of patterning graphene. It is completely adaptable to desired patterns, great resolution of feature sizes, and incorporates a common process semiconductor process.

4.2 Graphene Transfer

4.2.1 Introduction to Transfer Methods

Graphene has attracted much attention for flexible electronics due to its high flexibility and electrical conductivity properties. Recently methods for fabricating large scale, layers of graphene using chemical vapor deposition (CVD) have been successful. But for graphene to be integrated into practical flexible electronics, the graphene must be transferred to an appropriate flexible substrate. Most degradation in graphene quality occurs during the transfer process, this is when tearing and ripping of the graphene typically occurs. A reliable graphene transfer of a small graphene pattern was needed for our research and this presented a multitude of problems that had to be solved.

When Andre Geim and Kostya Novoselov first isolated the atomically thin film of graphene in 2005, it was by mechanical exfoliating a thin piece of graphite from highly oriented pyrolytic graphite with Scotch tape [18], as shown in Figure 11. Because graphite is just graphene layers stacked into a 3-dimensional structure, peeling layers with scotch tape repeatedly will eventually lead to a very thin piece of graphene. However mechanical

exfoliation does not quite constitute transfer since it is more of a method of obtaining graphene, but it does lead to the roll-to-roll transfer method.

Roll-to-roll is a process seen in the paper or metal rolling industry where two rollers spin together while applying pressure and heat to the material in-between.

This process is easily scalable and allows for the continuous production of the desired material. A CVD

graphene is grown on a rounded copper foil, and is attached to thermal release tape. A Cu etchant is used to remove the copper, leaving the graphene on the thermal tape. The graphene is transferred onto a flexible substrate by simply moving it between two rollers that are heated at 120 degrees Celsius. The heating removes the adhesiveness of the thermal tape and the released graphene adheres to the flexible substrate shown in Figure 12. Using this method it is possible to accomplish layer-by-layer stacking of graphene.

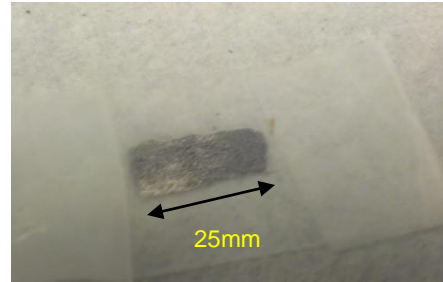


Figure 11: Scotch tape method of obtaining graphene.

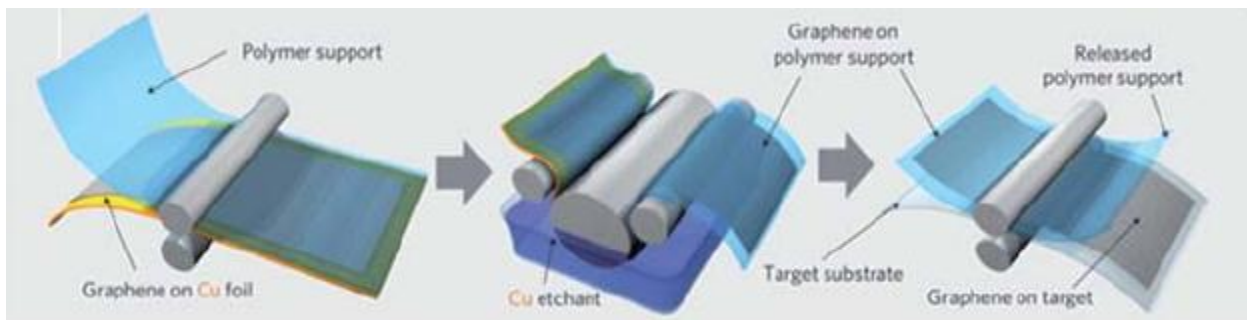


Figure 12: Roll to Roll transfer. (26)

As mentioned previously, the transfer process is where graphene incurs the most damage. The roll-to-roll method can leave residues and any physical transfer can cause ripping or tearing. Because of these issues, development of a transfer-free process is generating much interest. The

idea is to grow graphene directly on the desired substrate that the graphene would have been transferred onto after synthesis. Different target substrates dictate a different method of transfer. While each technique differs in details, they all try to solve the problems of transferring graphene.

Polymer support transfer methods are closely tied with CVD graphene. The metal substrate that the graphene is grown on is unwanted after successful synthesis and is removed. Common metal substrates, nickel and copper, can be etched with FeCl_3 (ferric chloric acid) [9]. The Hong group reported a wet etching transfer method of CVD graphene onto a silicon oxide substrate [9]. However the graphene was very thin and therefore tore and ripped easily during the transfer and etching. For this reason many researchers also report a dry transfer method. [26]. Polymer support has made large scale graphene transfers possible. PDMS (Polydimethylsiloxane) was one of the first polymers to be used for CVD graphene transfer. PDMS is a moldable, durable, unreactive, hydrophobic, and solvent resistant material that is commonly used in soft lithography [47]. The most significant characteristic is the low surface free energy, between 20 and 30 mN/m [48]. In a soft lithography process, the material to be lithographed, “stamped”, onto a substrate is applied to PDMS cast into desired pattern and shape [49]. PDMS maintains a low adhesion force with the stamped material, this means when the material comes into contact with the target substrate, it will adhere to the substrate rather than the PDMS, therefore the material is released from the PDMS and stamped onto the substrate. This is the working mechanism for graphene transfer [9]. The PDMS acts as a support to the graphene during the metal etching. After this the freed graphene on PDMS is brought to contact with the target substrate, and soft lithography occurs and the graphene is released from PDMS and transferred to the substrate with the higher surface free energy, as shown in Figure 13. However

the metal etching process is extremely slow, this is because only a thin layer of metal is exposed to the etchant.

PDMS has also shown success in the usage of graphene device manufacture. PDMS stamping nano fabrication has made the process of not rupturing patterned graphene relatively simple. Kang et al. has shown successful device fabrication by molding PDMS with the desired pattern [50]. After etching away the metal, only the graphene that was adhered to the PDMS pattern remain. The graphene was then stamped onto a target substrate.

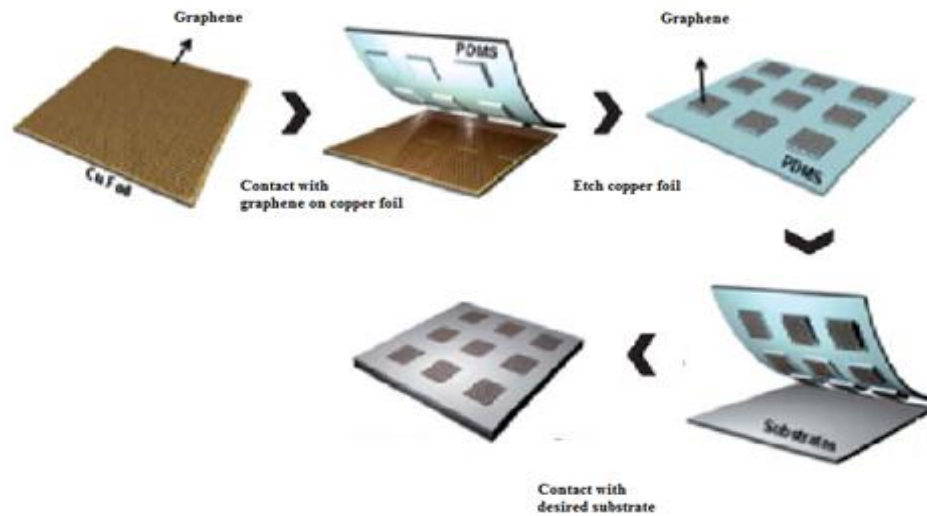


Figure 13: Dry Stamp Transfer Method. (50)

PMMA (polymethyl methacrylate) is another common polymer used in CVD graphene transfers. PMMA is spin coated onto CVD graphene grown on a metal [51], the metal is then etched away freeing the PMMA with graphene. This PMMA/graphene layer is deposited on a desired substrate, and the PMMA layer is removed with acetone. However PMMA is likely to cause cracks and rips in the graphene and PMMA is not always completely washed away with acetone and leaves residue, making this not an ideal method for obtain good quality graphene

transfer. Even with all the drawbacks of PMMA and PDMS transfers, they are still heavily used because of their reliability and familiarity.

There are many ways of transferring graphene to the desired substrate, and while each method is different, they all try to reduce physical damage and minimize the disturbances of the electrical properties from the transfer. However each method has its advantages and disadvantages. Mechanical exfoliation may avoid etchants and polymers but induces heavy physical damage; transfer-free methods are very substrate specific and difficult to adapt; and polymer support leaves unwanted residues.

Determining the flexible substrate to be used for our sensor was the first crucial step. PDMS (Polydimethylsiloxane) was selected mainly because it has strong Van der Waal forces; this ensured good transmittance of the strain through the PDMS to the graphene and good attraction of graphene to PDMS. PDMS was also attractive as a choice due to its availability in the lab, ease to work with, and various other properties [52]. While not an initial consideration, but PDMS can be bonded easily and this was an important factor in the ability to stack single graphene sensors.

Graphene transfers can be done by two major techniques: wet transfer or dry transfer.

Wet method involve the use of a liquid solution to remove the initial substrate that graphene is grown or deposited on [53]. The substrate etching solution has no effect on the graphene, therefore only the initial substrate is etched away leaving only graphene on the PDMS substrate. A liquid mixture of PDMS and curing agent (PDMS: curing agent = 15:1) was poured on the surface of the graphene-Ni foil. This PDMS: curing agent ratio was determined to have the maximum efficient bonding force to graphene and cured percentage of PDMS for ease of workability [52], [54]. The PDMS mixture next was placed into a vacuum chamber for 60

minutes to remove the air bubbles trapped in the PDMS and then cured on a hot plate at 90 degrees Celsius for 1 hour. Next the PDMS-graphene was placed in a metal etching solution, FeCl₃ (~0.1 g/ml) was used to etch the nickel substrate, and the etching process typically took 24 hours. Once the nickel was etched away this left the graphene on the flexible PDMS substrate. However this wet transfer process has a major issue, the PDMS would undercut the graphene and cover the underside of the graphene preventing metal etching, as shown in Figure 14.

Dry method involves the use of a PDMS stamp to lift off a layer or layers of graphene from its initial substrate shown in Figure 14. This method uses the attraction forces and cross-linking properties of graphene and PDMS to separate the graphene layers, however this method can only be used on multi-layer graphene as the graphene to PDMS force is greater than the graphene to graphene attraction forces [53]. A PDMS stamp was made by mixing PDMS and curing agent with a ratio of 10:1, as mentioned above this ratio was determined to have the best characteristics needed for graphene transfer. The liquid mixture was then put into a vacuum chamber for 60 minutes to remove any air bubbles trapped in the PDMS. Next the PDMS was cured on a hot plate for 1 hour at 90 degrees Celsius to create the PDMS stamp. The stamp was then attached to the graphene and slowly peeled off from the nickel substrate. This resulted in graphene layers being transferred onto the PDMS stamp surface because the adhesion force of PDMS-graphene is higher than the force between the graphene layers. By adjusting the ratio of PDMS and curing agent, it was possible to determine the adhesion force between the PDMS and target substrate, meaning it was possible to control how many layers of graphene were transferred onto the PDMS [55].



Figure 14: Result of a Wet Etch transfer and A Wet Peel Transfer.

4.2.2 Step 1: PDMS Graphene Transfer

A transfer method that combined both wet and dry methods was developed, and this allowed for the utilization of the advantages of both methods as shown in Figure 17. The use of a PDMS stamp was used as a substrate and a nickel etching solution of ferric chloric acid was used to etch away the initial nickel substrate in a wet transfer.

A PDMS stamp was made by mixing PDMS and curing agent with a ratio of 15:1, as mentioned above this ratio was determined to have the best characteristics needed for graphene transfer. The liquid mixture was then put into a vacuum chamber for 60 minutes to remove any air bubbles trapped in the PDMS from the mixing process. By removing any air bubbles it ensured that the fabricated PDMS stamp would be smooth for best surface adhesion to the graphene. Next the PDMS was poured on a glass slide to create a flat smooth surface and then it was cured on a hot plate for 1 hour at 75 degrees Celsius to create the PDMS stamp. At this temperature and time period, it ensured that the PDMS stamp was cured enough to work with as a stamp yet maintained enough tackiness to adhere to the graphene [56]. If the PDMS was cured at too high of a temperature, this decreased the cross-linking of PDMS to graphene and the flexibility of the stamp is decreased. If the PDMS was cured at too low of a temperature, the

PDMS would under-cure and formed a gel instead of a stamp. These effects also occurred at a time period that is too long or too short. The flat smoothness of the PDMS stamp is of crucial importance to ensure good surface to surface bonding between the graphene and the PDMS. The PDMS stamp was fabricated on a glass slide to make sure the stamp was a smooth flat surface.

Once the PDMS stamp was created, it needed to be attached to the patterned graphene. Make sure the graphene is flat and on a solid flat surface, slowly attach PDMS stamp smoothly onto the graphene. Apply pressure on the PDMS stamp to ensure good adhesion to graphene and to remove any air trapped between the two. Once the PDMS stamp was well attached to the patterned graphene it was then placed into the metal etching solution, as shown in Figure 15.

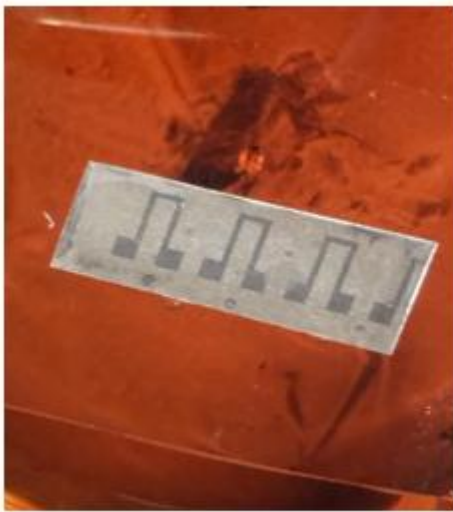


Figure 15: Graphene/Ni in metal etching solution.

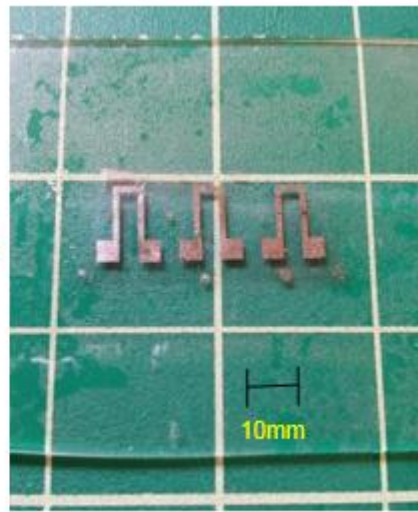
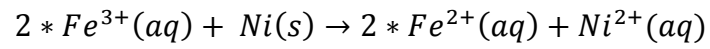


Figure 16: Graphene successfully transferred onto PDMS.

4.2.3 Step 2: Etching Initial Nickel Substrate

The nickel etching solution was a ferric chloride solution that was prepared with 27 grams of ferric chloride and 300 ml of DI water or (~ 0.1 g/ml). The PDMS/graphene/Ni slab was placed into the etching solution for 24 hours until the Ni was etched completely away, as shown in Figure 16.

An aqueous iron (III) chloride (FeCl_3) solution (1 M) was used as an oxidizing etchant to remove the nickel substrate. The net ionic equation of the etching reaction is:



Graphene Transfer Process

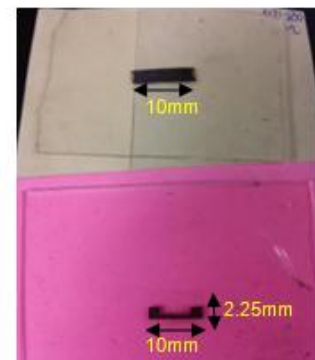
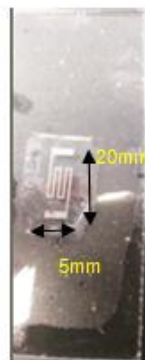
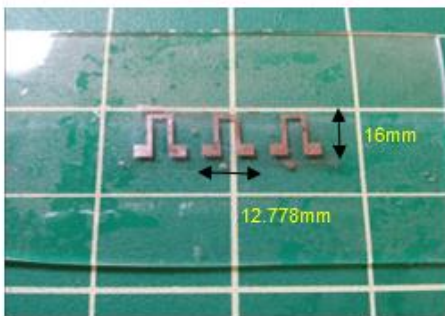
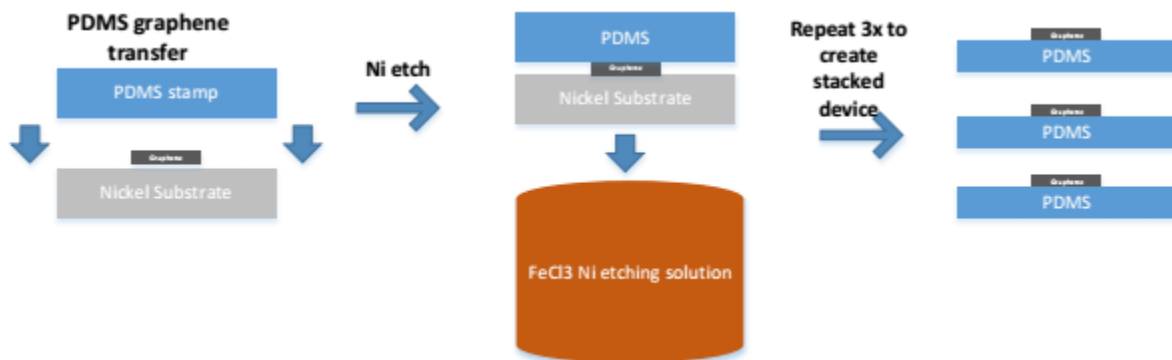
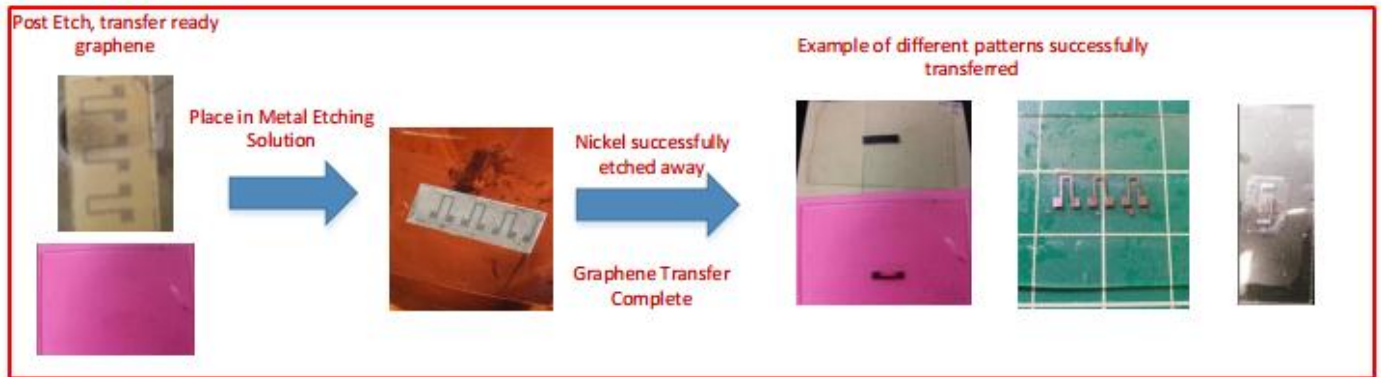


Figure 17: Images showing the transfer process and the different patterns that could be fabricated.

4.2.3 Raman Spectroscopy Tests

Raman spectroscopy is an important part of graphene research. It can be used to determine the number of layers of graphene present, the quality and type of graphene, and the effects that strain, doping, stress, electric and magnetic fields have on graphene [57]. Raman spectroscopy is the ideal tool that provides fast, high resolution, non-destructive characterization of graphene [58]. The use of Raman was used in our research to confirm the successful transfer of graphene and to obtain an estimation of how many layers of graphene were transferred.

Raman spectroscopy is a spectroscopy method that uses the inelastic scattering of monochromatic light, typically from a laser light source. This technique is named after Professor C. V. Raman, who discovered the Raman Effect in 1928 [59]. This technique is used to observe rotation, vibration, and other low frequency modes in a system [60]. The principle is based on the interaction of monochromatic light with a given sample. The sample absorbs the photons of the laser light and then reemitted. Frequency of the reemitted photons are shifted up or down compared to the original monochromatic frequency. This shift, the Raman Shift, provides information about the aforementioned frequency transitions in molecules. The Raman Effect is based on molecular deformations in the electric field E which is determined by, the molecular polarizability.

Raman scattering on phonons is determined by the movement, interference, and scattering of the electrons. Variations in the electrical properties due to doping, edges, defects, or magnetic fields will affect the positioning, width, and intensities of the Raman peaks.

There are three main peaks of phonon scattering in graphene that detail important properties. At a frequency around 1550 cm^{-1} there is a peak called the G peak which is observable in all carbon materials, and only the optical phonon with zero momentum is present at

this specific frequency. A 2D peak with frequency around 2700 cm^{-1} is indicative of second order Raman scattering. This 2D peak is the resonant scattering in which the incident photon energy coincides with the real energy band. The fewer layers of graphene that are present, the sharper the 2D peak will be at 2700 cm^{-1} . The sharpness of the 2D peak for our graphene indicates there are at most 10 layers of graphene present. If defects are present in the graphene, this may lead to the “D” peak. Figure 18 provides the plots detailing these peaks.

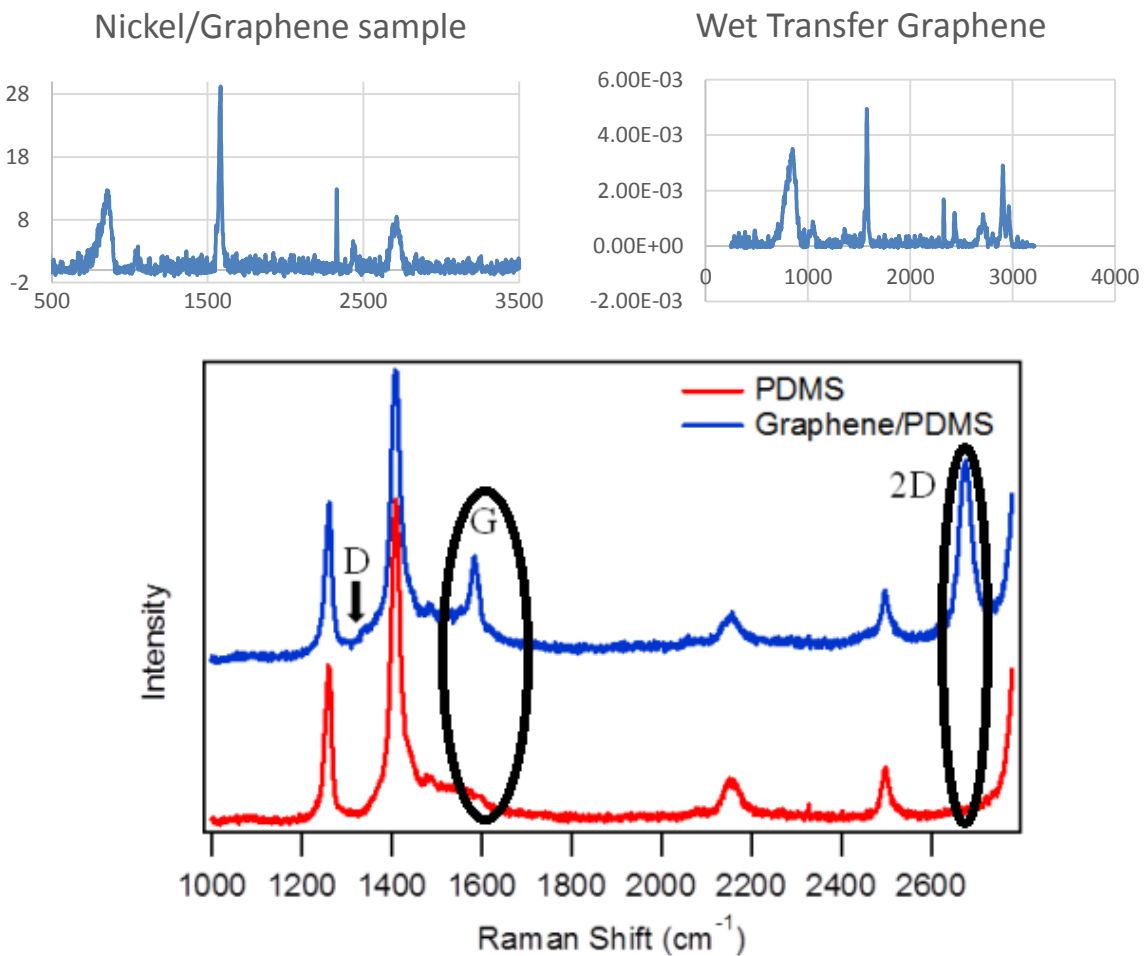


Figure 18: Comparison of the peaks, providing evidence of successful graphene transfer.

4.4 Flexible Graphene Sensors

4.4.1 Single Graphene Sensor

A strain gauge is a device that measures strain. It works by having a flexible backing that supports a metallic foil pattern. This gauge is attached to an object and as that object is deformed, the foil also undergoes deformation which caused the electrical resistance to change. Instead of a metal foil, the patterned graphene is the resistance changing element in the sensor. A single graphene sensor consisted of a pattern graphene resistor attached to a PDMS substrate. As strain is applied with a tensile bench to the graphene, the resistance can be measured with a multi-meter. Results show that as strain is applied, the resistance shows a linear trend of increase with the strain applied. However a single resistor is limited in its real-world applications.

To improve the robustness and stability of our graphene contacts during strain testing, liquid metal was injected to reinforce the contact areas. This prevented the graphene contacts from deteriorating when strain was applied during testing. The liquid metal also had the added benefit of enabling our device to maintain flexibility and made measurements of the different layers of the device easier.

4.4.2 Stacked Rosette Strain Sensor

In the field of strain sensing, the rosette pattern is commonly used because it allows for multi-directional strain sensing. A strain gauge rosette is an arrangement of two or more closely positioned gauges. In common cases where the principal directions of strain are unknown, all it takes is three independent strain measurements (all of different directions) to determine the principal strains or vice versa. However where most devices have a planar rosette pattern, due to the flexibility of graphene, it is possible to stack our devices to form the rosette pattern and this is advantageous over current planar rosette sensors. A stacked rosette minimizes sensor size yet

is still able to measure multiple directions and magnitudes of stress to a very precise point. In traditional MEMS sensor fabrication with silicon, a stacked device is infeasible due to the rigidity of the material. Graphene on the other hand is as flexible as the flexible substrate is it

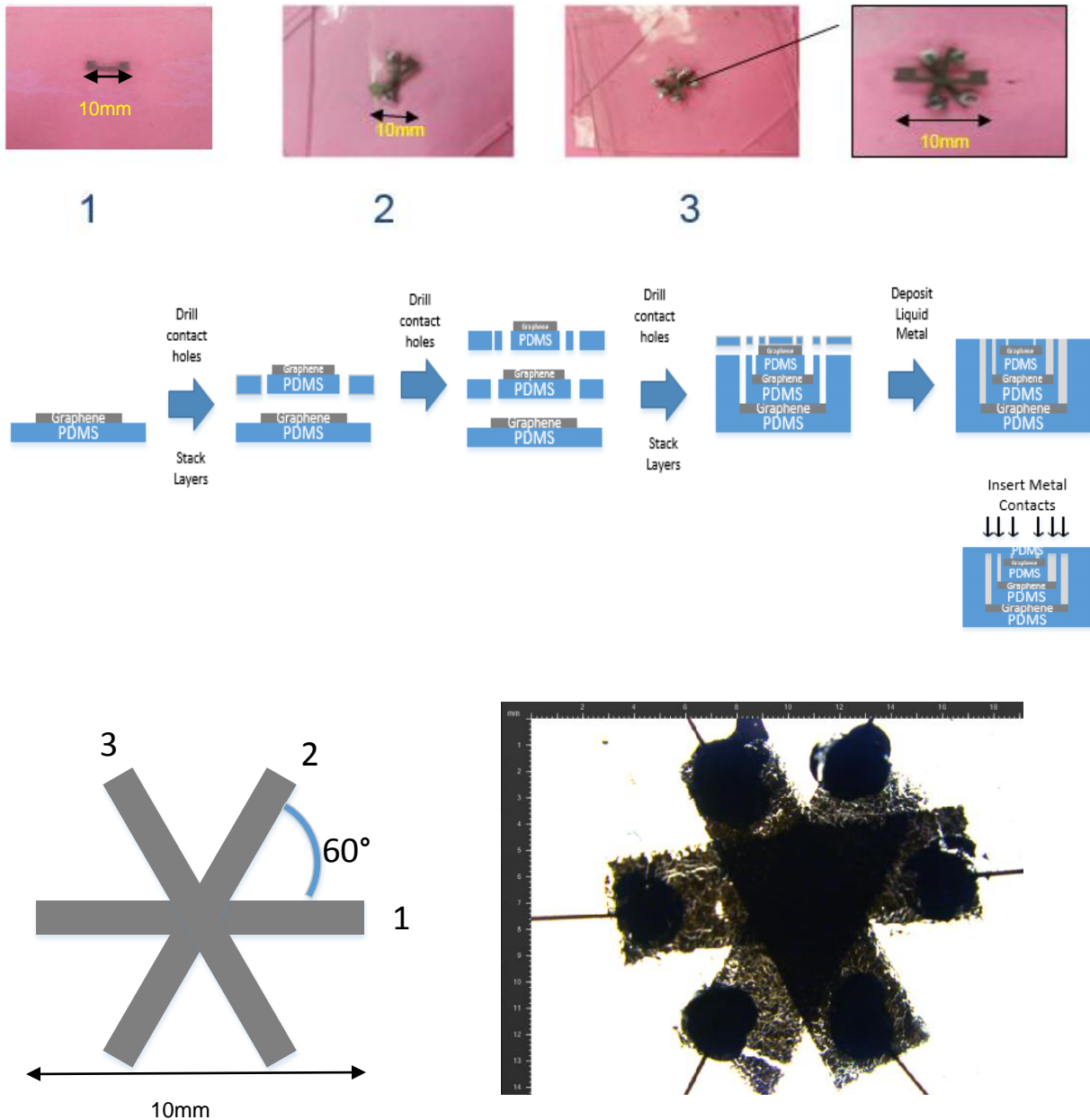


Figure 19: Final Design: Stacked Rosette Graphene Sensor.

CHAPTER 5: DEVICE PERFORMANCE AND RESULTS

5.1 Piezoresistive Effect

To test the theory that graphene will change resistance when strain applied and it is a consistent and repeatable method for measuring resistance changes, our device was put on a strain stage that enabled us to apply controlled strain. Also required was to test whether this fabrication and transfer process produces a graphene pattern that will perform as expected. First to check the graphene pattern for completeness of patterning, transfer and connectivity, strain was applied to the graphene using a tensile stage and resistance change was measured using a multimeter. As can be seen in Figure 20, there is a linear correlation between the applied strain and change in resistance in the graphene. Deviations from this linear pattern occur when the graphene in the sensor is stretched past a certain point in which the graphene starts to break and tear.

The piezoresistive properties of graphene were tested by applying strain to a single graphene resistor. The van der Waals force between PDMS and graphene provide a strong adhesion and therefore the strain experienced by the PDMS is also experienced by the graphene. To measure the piezoresistivity, the PDMS with graphene sensor is stretched along a uniaxial direction at small increments 0.1mm (~0.01%). During the stretching, a multimeter was applied to the graphene strain sensor to measure the change in electrical resistance. In a neutral, no strain, position the distance between the two fixed ends was 10mm (0%) and at max strain the ends was measured at 11mm (10%). Throughout the test, the electrical resistance was continuously measured as a function of applied strain. As shown in Figure 20, as the strain applied increased, so did the resistance in a *linearly* fashion. The graphene sensor does show good repeatability, the sensor underwent multiple trials of stretching and un-stretching and the

electrical resistance was continuously measured. Figure 20 shows that the sensor showed good consistency in measuring the relationship of applied strain to electrical resistance and through that the relationship of applied strain and current. Typical electrical resistance of a commercial semiconductor strain gauge is 1kOhms.

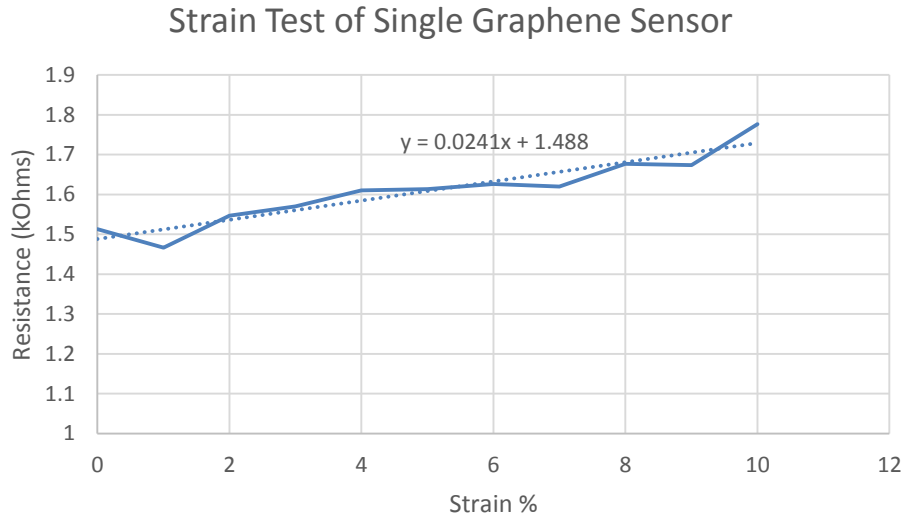


Figure 20: Strain Test of a Single Graphene-based Sensor

5.2 Rosette Design for Multi-Directionality

A single graphene based strain sensor is only capable of detecting strain or deformation in a singular direction. This limits the usefulness of the sensor in real-life applications. For characterization of complicated multi-directional deformations on a surface, it is necessary to measure strain in three dimensions, eX , eY , $e\theta$. To accomplish this, three of the same strain sensors are arranged to form a rosette, each sensor oriented at 120 degrees from each other forming an equilateral triangle formation. The placement of three equally spaced strain sensors, each with a fixed 60 degree angle from each other, is called a planar 60-delta rosette gauge system, as shown in Figure 21 and 23. The strain sensors in the rosette arrangement are named

x, y, and z and their corresponding strain values ϵ_x , ϵ_y , and ϵ_z . By using the measured magnitudes of strain and the directions of the gauges, it is then possible to determine the full strain on the surface of the sensor location. The Mohr's circle, better known as the "strain transformation method", can graphically illustrate the surface state of strain Figure 22 (noting that the angles in Mohr's circle are double the physical angles on the test surface). The strain at any angle θ from the major principal axis can be expressed as:

$$\text{Strain} = (eX + eY)/2 + (eX - eY)/2 * \cos(2\theta) \quad \text{Eq. 3}$$

The strain on each rosette gauge can be represented in terms of principal strain on x and y axis with corresponding rotation angles θ , $\theta + 60$ degrees, and $\theta + 120$ degrees. Using the following strain transformation equations it is possible to determine the directionality of the strain applied.

$$\epsilon_x = \frac{eX+eY}{2} + \frac{eX-eY}{2} * \cos(2\theta) \quad \text{Eq. 4}$$

$$\epsilon_y = \frac{eX+eY}{2} + \frac{eX-eY}{2} * \cos 2(\theta + 60^\circ) \quad \text{Eq. 5}$$

$$\epsilon_z = \frac{eX+eY}{2} + \frac{eX-eY}{2} * \cos 2(\theta + 120^\circ) \quad \text{Eq. 6}$$

We can measure the strain values of ϵ_x , ϵ_y , and ϵ_z , and with those values it is possible to calculate the principal strain values x and y, and their orientation θ with the following equations.

$$eX, Y = \frac{\epsilon_x + \epsilon_y + \epsilon_z}{3} + / - \frac{\sqrt{2}}{3} * \sqrt{((\epsilon_x - \epsilon_y)^2 + (\epsilon_y - \epsilon_z)^2 + (\epsilon_z - \epsilon_x)^2)} \quad \text{Eq. 7}$$

$$\theta = \left(\frac{1}{2}\right) \tan^{-1} \left(\frac{\sqrt{3} * (\epsilon_y - \epsilon_z)}{2\epsilon_x - \epsilon_y - \epsilon_z}\right) \quad \text{Eq. 8}$$

[64]

The "+/-" in Eq. 7 is used to calculate the maximum and minimum principle strain, respectively, in Mohr's circle.

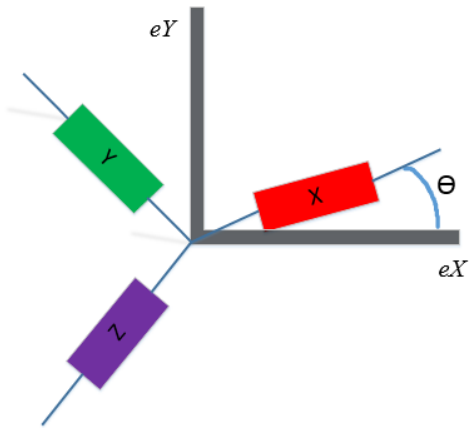


Figure 21: Direction of principal strain in a Rosette pattern.

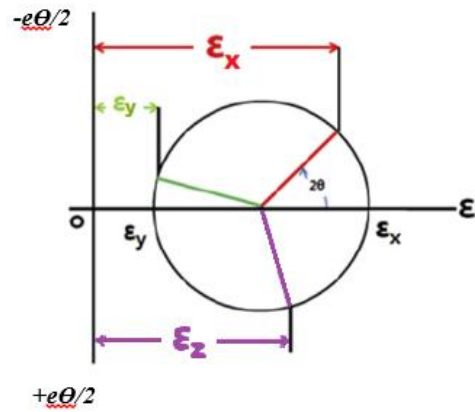


Figure 22: Mohr's circle diagram for strain analysis. Rosette axis superimposed on Mohr's circle for strain.

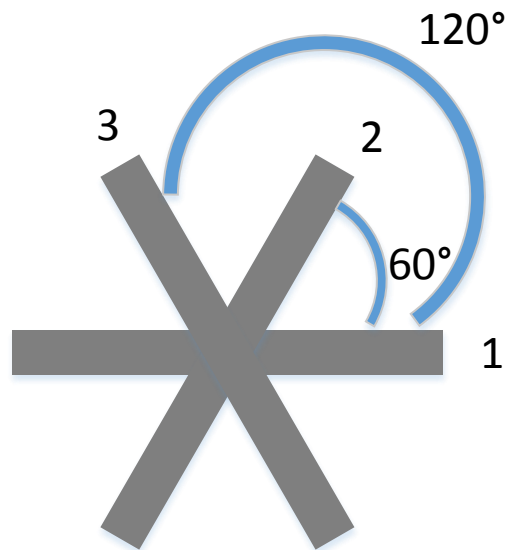


Figure 23: Delta rosette.

5.3 Stacked Multi-Layered Device

Additionally, the rosette-type strain sensor was made up of 3 stacked devices instead of planar devices arranged in a rosette shape. The major disadvantage to a planar rosette is the larger surface area covered. Whereas a stacked rosette will occupy the least amount of area and has the center of all the gauges lying over the same point on the surface. Therefore a stacked rosette has better accuracy on strain measurements. The strain sensing device combines the multi-directional measuring abilities of a rosette pattern and it also improves upon this design by stacking the devices for better size management and signal resolution.

The strain sensing characteristics of the rosette shaped stacked device was investigated by the same method as that of the single graphene strain device, however now the resistance change of the three strain sensors was measured. Figure 24, 25, and 26 shows the measurement of the resistances as a function of the applied strain for all three strain gauges. The stretching was applied along the x-axis, such that the 'x' gauge and the other two gauges were positioned at the same distance and oriented at the same angles with respect to the 'x' gauge. It was measured that as the strain was increased to the sensors, the resistances measured also increased. As previously discussed, with the values of the strain on the three strain sensors known, the principal strain and their orientation with respect to the rosette axis can be estimated. The robustness of the device was tested by performing the strain test several times. Figure 25 shows the measurements of the three strain sensors, and it shows the change in the resistance repeated in the repeated strain tests. This verified that the fabricated rosette graphene strain device has a very robust capability of sensing strain.

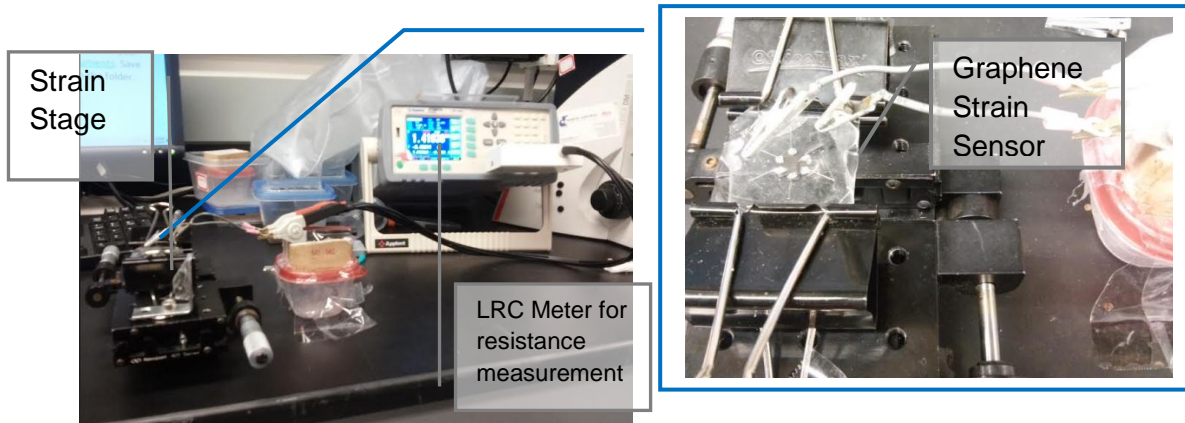


Figure 24: Strain Testing Setup.

The plots, shown in Figure 25 and 26, show the relationship between resistance and strain. As strain is increased, the resistances of the strain sensors linearly increase. Variations in the linear relation are due to breakage in the graphene and uneven stretching of the PDMS substrate. If there is a slight drop in resistance this is due to ripples in the graphene that are evening out as strain is applied. The stacked design of the sensor also contributes to the slight variations in resistance responses to the strain. But as the resistance plots shows, the sensors show similar and consistent responses to the same applied strain.

Each individual sensor was characterized, shown in Figure 25, a constant and consistent application of strain was applied to the device and the resistance for each sensor was measured. Strain values for sensors 1, 2, and 3 from this resistance-change data is calculated to 10%, 2.67%, and 2.67%, when the principal strain of about 10% is applied in the X-direction. As previously discussed, when the values of the three independent strains from the three sensors is known, the principal strains and their orientations with respect the rosette axis can be estimated. The principal strains eX and eY and their angle of orientation are calculated by inserting the three strain values of the three sensors into Eq. 7 and 8 and are found to be 10%, 0.22%, and 0° ,

respectively. The calculated value of 10% for maximum principal strain (e_X) matches the applied strain value, and this is indicative of good accuracy and sensing capability of the stacked graphene rosette strain sensor. The change in resistance characteristics repeated multiple times as the gradual increase and decrease of applied strain, and this verified that the fabricated stacked rosette graphene sensor showed a stable capability of sensing strain under repeated measurements.

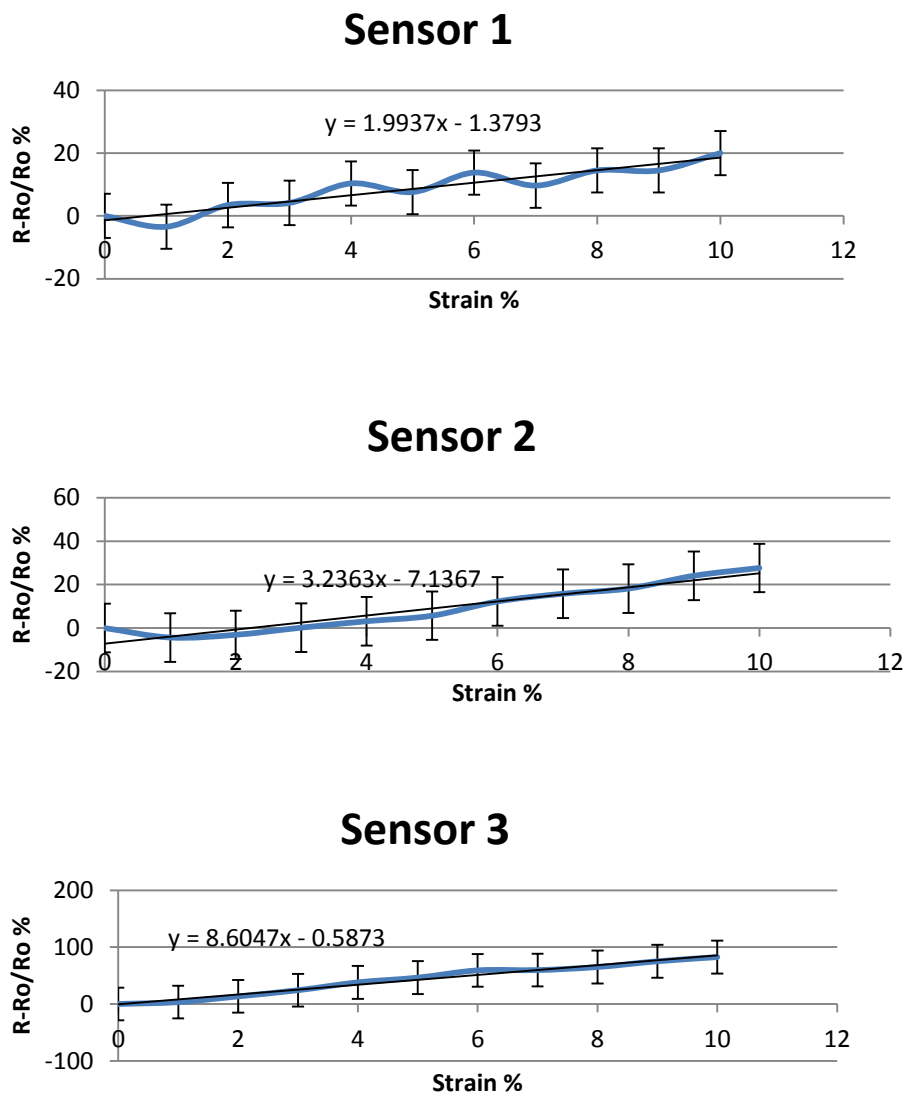
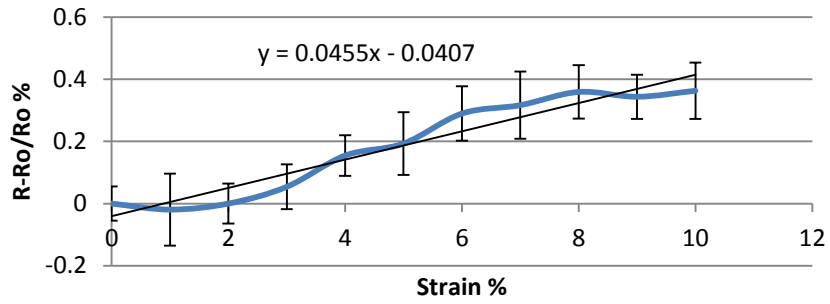
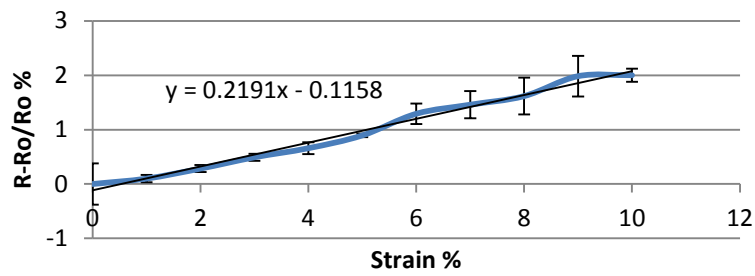


Figure 25: Sensor Characterization.

Sensor 1



Sensor 2



Sensor 3

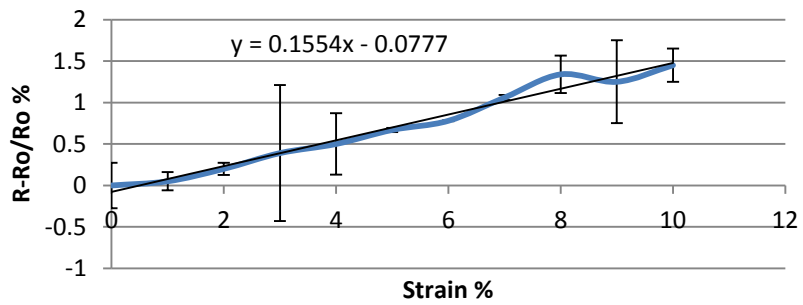


Figure 26: Multi-layer rosette strain plots measuring strain applied in Sensor 2 direction.

The angle of the direction of applied strain was also varied to test the ability of the sensor to measure the directionality of our graphene sensor. The device was rotated so that the direction of applied strain was in the same line as sensor 2 and the resistance was measured as strain was applied like before, shown in Figure 26. The strain values for sensors 1, 2, and 3 were measured as 2.67%, 10%, and 2.67% respectively. Using these strain values and Equations 7 and 8, the principal strains eX and eY and their angle of orientation are calculated to be 10%, .22%, and -30°, respectively. The calculated value of 10% for maximum principal strain (eX) matches the applied strain value, however the angle was different from the expected value. Possible explanations for this is that during set-up the device was not rotated fully and so strain was not perfectly in-line with sensor 2, another explanation is that the calculations are correct and that our expected value is incorrect. This test does show that the strain sensor can detect variations of direction of applied strain and that it still accurately measures the principle strain values.

Our tests show that graphene is a viable material to be used in strain sensors, but how does it compare to the current material standard of silicon. Typical silicon based commercial strain sensors have an electrical resistance of 1 ohms; our sensor had an electrical resistance of about 1.5 ohms. Gauge factor indicates the relation between the change in electrical resistance and the applied strain: as shown above in equation 2. The resistivity change for a metal is typically of the order of 0.3, which is smaller compared to a semiconductor such as silicon which is 50-100 times larger. For graphene the gauge factor is approximately 1.4-2.0. Lastly the measure of cross-sectional area of material reduces in proportion to the longitudinal strain is Poisson's ratio. For most metals Poisson's ratio ranges from 0.20 to 0.35, for silicon it is about 0.28, and for graphene it is about 0.165.

Table 3: Graphene versus Silicon

	Single graphene sensor electrical resistance	Gauge factor	Possion's ratio
Graphene	~1.5 kohms	1.4-2	~0.168
Silicon	~1 kohms	-125 - +200	~0.28

The sensitivity per unit area of graphene sensors is about 20 to 100s of times higher than that of conventional piezoresistive pressure sensors. These results show that graphene is a viable replacement for silicon in strain sensors.

CHAPTER 6: CONCLUSION AND FUTURE WORK

6.1 Conclusion

This thesis presented methods of patterning and transferring graphene and demonstrated the successfulness of these methods by fabricating a stacked graphene rosette strain sensor. We have shown that the properties of graphene are useful for electronic and sensing applications. Both theoretical and experiment reports indicate that graphene is a viable candidate for flexible sensor applications. A graphene based piezoresistive strain sensor was fabricated by integrating graphene resistors on a flexible PDMS substrate. A reliable method of patterning graphene into a desired pattern and a method for transferring that graphene onto a flexible substrate was also developed. The use of graphene for high performance pressure sensor applications was demonstrated by the characteristics of the piezoresistive effect of graphene and the sensitivity of graphene to strain and pressure. Graphene's intrinsic flexibility, it allows for successful fabrication of a stacked device in a rosette pattern. Therefore a strain device in this configuration is able to detect magnitude and direction of principal strains in three dimensions and in a small device.

6.2 Future Work

The development of a reliable method of graphene patterning and transfer, this allows for stable isolation of graphene on a flexible substrate. These methods can be utilized in the fabrication of different types of graphene sensors and in the field of wearable electronics. Sensitivity of the graphene sensor can be further improved by integrating a full Wheatstone bridge into the graphene based sensing device. A Wheatstone bridge will increase the sensitivity of the graphene resistor allowing it to detect even smaller changes in strain.

REFERENCES

- 1: Lundstrom, M. (2003). APPLIED PHYSICS: Enhanced: Moore's Law Forever? *Science*, 210-211.
- 2: Geim, A. Graphene: Status And Prospects. *Science*, 1530-1534.
- 3: Novoselov, K., Fal'ko, V., Colombo, L., Gellert, P. A roadmap for graphene. *Nature*, 192-200.
- 4: Chen, J., Jang, C., Xiao, S., Ishigami, M., & Fuhrer. Intrinsic and extrinsic performance limits of graphene devices on SiO₂. *Nature Nanotechnology*, 206-209.
- 5: Lee, C., Wei, X., Kysar, J., & Hone. Measurement Of The Elastic Properties And Intrinsic Strength Of Monolayer Graphene. *Science*, 385-388.
- 6: Loh, K., Bao, Q., Ang, P., & Yang, J. The chemistry of graphene. *Journal of Materials Chemistry*, 2277-2277.
- 7: Lee, Y., Bae, S., Jang, H., Jang, S., Zhu, S., Sim, S. (2010). Wafer-Scale Synthesis and Transfer of Graphene Films. *Nano Letters*, 490-493.
- 8: Fu, X., Liao, Z., Zhou, J., Zhou, Y., Wu, H. Strain dependent resistance in chemical vapor deposition grown graphene. *Applied Physics Letters*, 213107-213107.
- 9: Kim, K., Zhao, Y., Jang, H., Lee, S., Kim, J., Kim, K., Hong, B. (2009). Large-scale pattern growth of graphene films for stretchable transparent electrodes. *Nature*, 706-710.
- 10: Novoselov, K. (n.d.). Electric Field Effect In Atomically Thin Carbon Films. *Science*, 666-669.
- 11: Mouras, S., Hamm, A., Djurado, D., *Revue de Chimie Minerale* 24(5), 572-582 (1987)
- 12: Dresselhaus, M., Dresselhaus, G., & Saito, R. (n.d.). Carbon fibers based on C₆₀ and their symmetry. *Physical Review B*, 6234-6242.
- 13: A. H. Castro Neto, F. Guinea, N. M. R. Peres, K. S. Novoselov, and A. K. Geim. The electronic properties of graphene. *Rev. Mod. Phys.* 81, 109
- 14: J. N. Fuchs and M. O. Goerbig. Introduction to the Physical Properties of Graphene. *Nano physics*, 2008
- 15: Mermin, N., & Wagner, H. (n.d.). Absence of Ferromagnetism or Antiferromagnetism in One- or Two-Dimensional Isotropic Heisenberg Models. *Physical Review Letters*, 1133-1136.
- 16: Wee, A. (2012). Graphene: The Game Changer? *ACS Nano*, 5739-5741.
- 17: Geim, A., & Novoselov, K. (n.d.). The Rise of Graphene. *Nature Materials*, 183-191.

- 18: Novoselov, K. (n.d.). Electric Field Effect in Atomically Thin Carbon Films. *Science*, 666-669.
- 19: Kwon, S., Bae, W. and Kim. Korean Journal of Chemical Engineering, 21, 910-914.
- 20: Saito, R.; Dresselhaus. Physical properties of carbon nanotubes; Imperial College: London, 1998.
- 21: Zhou, S., Gweon, G., Graf, J., Fedorov, A., Spataru, C., Diehl, R., Lanzara, A. (2006). First direct observation of Dirac fermions in graphite. *Nature Physics*, 595-599.
- 22: Bolotin, K., Sikes, K., Jiang, Z., Klima, M., Fudenberg, G., Hone, J., Stormer, H. (n.d.). Ultrahigh electron mobility in suspended graphene. *Solid State Communications*, 351-355.
- 23: Murali, R., Yang, Y., Brenner, K., Beck, T., & Meindl, J. (n.d.). Breakdown current density of graphene nanoribbons. *Applied Physics Letters*, 243114-243114.
- 24: Meric, I., Han, M., Young, A., Ozyilmaz, B., Kim, P., & Shepard, K. (2008). Current saturation in zero-bandgap, top-gated graphene field-effect transistors. *Nature Nanotechnology*, 654-659.
- 25: Zhu, Y., Murali, S., Cai, W., Li, X., Suk, J., Potts, J., & Ruoff, R. (n.d.). Graphene-based Materials: Graphene and Graphene Oxide: Synthesis, Properties, and Applications (Adv. Mater. 35/2010). *Advanced Materials*.
- 26: Bae, S., Kim, H., Lee, Y., Xu, X., Park, J., Zheng, Y., Iijima, S. (2010). Roll-to-roll production of 30-inch graphene films for transparent electrodes. *Nature Nanotechnology*, 574-578.
- 27: Rafiee, M., Rafiee, J., Wang, Z., Song, H., Yu, Z., & Koratkar, N. (2009). Enhanced Mechanical Properties of Nanocomposites at Low Graphene Content. *ACS Nano*, 3884-3890.
- 28: Bogue, R. (n.d.). Nanosensors: A review of recent research. *Sensor Review*, 310-315.
- 29: Mohammed, A. Mechanical Strain Measurements Using Semiconductor Piezoresistive Material. *Nano and Smart Systems*, 2006
- 30: Sun, D., Aivazian, G., Jones, A., Ross, J., Yao, W., Cobden, D., & Xu, X. (2012). Ultrafast hot-carrier-dominated photocurrent in graphene. *Nature Nanotechnology*, 114-118.
- 31: Laukhina, E., Pfattner, R., Ferreras, L., Galli, S., Mas-Torrent, M., Masciocchi, N., Veciana, J. (2009). Ultrasensitive Piezoresistive All-Organic Flexible Thin Films. *Advanced Materials*.
- 32: Berger, C., Song, Z., Li, T., Li, X., Ogbazghi, A., Feng, R., Heer, W. (n.d.). Ultrathin Epitaxial Graphite: 2D Electron Gas Properties and a Route toward Graphene-based Nanoelectronics. *The Journal of Physical Chemistry B*, 19912-19916.

- 33: Hummers, W., & Offeman, R. (n.d.). Preparation of Graphitic Oxide. *Journal of the American Chemical Society*, 1339-1339.
- 34: Li, Y., Zhou, Z., Shen, P., & Chen, Z. (2009). Structural and Electronic Properties of Graphene Nanoribbons. *The Journal of Physical Chemistry C*, 15043-15045.
- 35: Li, X., Cai, W., Colombo, L., & Ruoff, R. (2009). Evolution of Graphene Growth on Ni and Cu by Carbon Isotope Labeling. *Nano Letters*, 4268-4272.
- 36: Apell, S. (n.d.). High optical absorption in graphene.
- 37: Multilayer Graphene on Nickel foil: 2"x2" (n.d.). Retrieved April 22, 2015, from <https://graphene-supermarket.com/Multilayer-Graphene-on-Ni-foil-2-x2.html>
- 38: Novoselov, K. (n.d.). Two-dimensional Atomic Crystals. *Proceedings of the National Academy of Sciences*, 10451-10453.
- 39: Girit, C., Meyer, J., Erni, R., Rossell, M., Kisielowski, C., Yang, L., Zettl, A. (2009). Graphene at the Edge: Stability and Dynamics. *Science*, 1705-1708.
- 40: Ebbesen, T., & Hiura, H. (n.d.). Graphene in 3-dimensions: Towards graphite origami. *Advanced Materials*, 582-586.
- 41: Bai, J., Zhong, X., Jiang, S., Huang, Y., & Duan, X. (n.d.). Graphene Nanomesh. *Nature Nanotechnology*, 190-194.
- 42: Chen, Z., Lin, Y., Rooks, M., & Avouris, P. (n.d.). Graphene nano-ribbon electronics. *Physica E: Low-dimensional Systems and Nanostructures*, 228-232.
- 43: Tapasztó, L., Dobrik, G., Lambin, P., & Biró, L. (2008). Tailoring the atomic structure of graphene nanoribbons by scanning tunnelling microscope lithography. *Nature Nanotechnology*, 397-401.
- 44: Han, M., Özyilmaz, B., Zhang, Y., & Kim, P. (n.d.). Energy Band-Gap Engineering of Graphene Nanoribbons. *Physical Review Letters*.
- 45: Dimiev, A., Kosynkin, D., Sinitskii, A., Slesarev, A., Sun, Z., & Tour, J. (2011). Layer-by-Layer Removal of Graphene for Device Patterning. *Science*, 1168-1172.
- 46: Al-Mumen, H., Rao, F., Li, W., & Dong, L. (2014). Singular Sheet Etching of Graphene with Oxygen Plasma. *Nano-Micro Letters*.
- 47: Lee, J., Park, C., & Whitesides, G. (n.d.). Solvent Compatibility of Poly(dimethylsiloxane)-Based Microfluidic Devices. *Analytical Chemistry*, 6544-6554.
- 48: S. J. Clarkson and J. A. Semlyen, *Siloxane Polymers*, Prentice Hall, Englewood Cliffs, NJ, 1993.

- 49: Gates, B., Xu, Q., Stewart, M., Ryan, D., Willson, C., & Whitesides, G. (n.d.). New Approaches to Nanofabrication: Molding, Printing, and Other Techniques. *Chemical Reviews*, 1171-1196.
- 50: Kang, S. J. *et al.* Inking elastomeric stamps with micro-patterned, single layer graphene to create high-performance OFETs. *Adv. Mater.* 23, 3531–3535(2011).
- 51: Reina, A., Jia, X., Ho, J., Nezich, D., Son, H., Bulovic, V., Kong, J. (n.d.). Large Area, Few-Layer Graphene Films on Arbitrary Substrates by Chemical Vapor Deposition. *Nano Letters*, 30-35.
- 52: Johnston, Mechanical characterization of bulk Sylgard 184. *Journal of Micromechanics and MicroEng*, 2014
- 53: Ko, P., Takahashi, H., Koide, S., Sakai, H., Thu, T., Okada, H., & Sandhu, A. (2013). Simple method to transfer graphene from metallic catalytic substrates to flexible surfaces without chemical etching. *Journal of Physics: Conference Series*, 012002-012002.
- 54: Kim, C., Woo, J., Choi, J., Park, J., & Han, C. (n.d.). Direct transfer of graphene without the removal of a metal substrate using a liquid polymer. *Scripta Materialia*, 535-537.
- 55: Chang-Soo Han, Direct Transfer of Graphene.
- 56: Yoo, K., Takei, Y., Kim, S., Chiashi, S., Maruyama, S., Matsumoto, K., & Shimoyama, I. (2013). Direct physical exfoliation of few-layer graphene from graphite grown on a nickel foil using polydimethylsiloxane with tunable elasticity and adhesion. *Nanotechnology*, 205302-205302.
- 57: Ferrari, A., Meyer, J., Scardaci, V., Casiraghi, C., Lazzeri, M., Mauri, F., Geim, A. (n.d.). Raman Spectrum of Graphene and Graphene Layers. *Physical Review Letters*.
- 58: Ni, Z., Wang, Y., Yu, T., & Shen, Z. (n.d.). Raman spectroscopy and imaging of graphene. *Nano Research*, 273-291.
- 59: Raman, C., & Krishnan, K. (1928). A Theory of the Optical and Electrical Properties of Liquids. *Proceedings of the Royal Society A: Mathematical, Physical and Engineering Sciences*, 589-599.
- 60: Venkataraman, G., & Ramdas, A. (n.d.). Journey into Light: Life and Science of C. V. Raman. *Physics Today*, 61-61.
- 61: Peplow, M. (2013). Graphene: The quest for supercarbon. *Nature*, 327-329.
- 62: Khoshnoud, F., & Silva, C. (n.d.). Recent advances in MEMS sensor technology-mechanical applications. *IEEE Instrumentation & Measurement Magazine*, 14-24.
- 63: Bae, S., Lee, Y., Sharma, B., Lee, H., Kim, J., & Ahn, J. (n.d.). Graphene-based transparent strain sensor. *Carbon*, 236-242.

64: Vishay. Strain Gage Rosettes: Selection, Application and Data Reduction.
<http://www.vishaypg.com/docs/11065/tn-515.pdf>

65: C.S. Smith, Piezoresistance effect in germanium and silicon. *Phys. Rev.*, 94 (1) (1954), pp. 42–49

66: X.-W. Fu, Z.-M. Liao, J.-X. Zhou, Y.-B. Zhou, H.-C. Wu, R. Zhang, *et al.* Strain dependent resistance in chemical vapor deposition grown graphene. *Appl Phys Lett*, 99 (21) (2011), p. 213107